Impact of secondary TCR engagement on the heterogeneity of pathogen-specific CD8$^+$ T cell response during acute and chronic toxoplasmosis

Lindsey A Shallberg[1], Anthony T Phan[1], David A Christian[1], Joseph A Perry[1], Breanne E Haskins[1], Daniel P Beiting[1], Tajie H Harris[3], Anita A Koshy[2], Christopher A Hunter[1]*

1. Department of Pathobiology, School of Veterinary Medicine, University of Pennsylvania, Hill Pavilion, 380 South University Avenue, Philadelphia, PA 19104-4539

2. Department of Neurology, Department of Immunobiology, and BIO5 Institute, University of Arizona, Thomas W. Keating Bioresearch Building, Rm 229, 1657 E. Helen Street, PO Box 210240, Tucson, AZ 85721-0240

3. Center for Brain Immunology and Glia, Department of Neuroscience, University of Virginia, 409 Lane Road, MR-4 Room 6148, Charlottesville, VA 22908

*Corresponding Author

Abstract

Initial TCR engagement of $CD8^+$ T cells results in T cell expansion, and these early events influence the generation of diverse effector and memory populations. During infection, some activated T cells re-encounter cognate antigen, but how these events influence local effector responses or formation of memory populations is unclear. To address this issue, OT-I T cells which express the Nur77-GFP reporter of TCR activation were paired with *T. gondii* that express OVA to assess the impact of TCR activation on $CD8^+$ T cell responses. During acute infection, TCR stimulation in affected tissues correlated with parasite burden and was associated with markers of effector cells while Nur77-GFP^- OT-I showed signs of effector memory potential. However, adoptive transfer of Nur77-GFP negative or positive OT-I from infected mice into naive recipients resulted in formation of similar memory populations. During the chronic stage of infection in the CNS, TCR activation was associated with large scale transcriptional changes and the acquisition of an effector T cell phenotype as well as the generation of a population of $CD103^+$ $CD69^+$ Trm like cells. However, while inhibition of parasite replication resulted in reduced effector responses it did not alter the Trm population. These data sets highlight the contribution of recent TCR activation on the phenotypic heterogeneity of the $CD8^+$ T cell response but suggest that this process has a limited impact on memory populations at acute and chronic stages of infection.

Author Summary

CD8$^+$ T cells are important to control many acute and chronic infections, however the role that recent T cell receptor stimulation plays in the formation of ongoing T cell responses is unclear. Here, we utilize a genetic reporter of TCR stimulation and high parameter flow cytometry to characterize TCR-driven phenotypes of pathogen specific T cell responses to the parasite *Toxoplasma gondii* during acute and chronic infection in the periphery and central nervous system. This work demonstrates the importance of recent TCR stimulation in driving local effector CD8$^+$ T cell responses in peripheral tissues during infection, as well as the plasticity of the formation of memory T cells. Additionally, we utilize static and live imaging to investigate how *Toxoplasma gondii* life cycle impacts the ability to present antigen to CD8$^+$ T cells. These studies aid in our understanding of how effector and memory CD8$^+$ T cell responses are generated and maintained during an infection.

Introduction

CD8$^+$ T cells play an important role in immunity to intracellular infections and multiple subsets including T effector, T memory, and T resident memory (Trm) cells have been associated with different anatomical locations and distinct functions [1-3]. During infection, dendritic cells in secondary lymphoid organs present microbially derived peptides via MHC Class I, activating T Cell Receptor (TCR) signaling of naive CD8$^+$ T cells. This signal 1, along with co-stimulation (signal 2) and cytokines (signal 3) induce a proliferative burst of CD8$^+$ T cells that results in 1,000 to 10,000 daughter cells produced from an individual CD8$^+$ T cell within a week of stimulation, which gives rise to diverse effector and memory populations [4-10]. After initial priming, CD8$^+$ T cells leave the secondary lymphoid organs and migrate to the periphery, where they can mediate TCR-dependent effector functions that include cytolysis of infected cells and secretion of cytokines (IFN-γ and TNF-α) required for resistance to infection. As pathogen burden is controlled there is a contraction phase where the majority of effector CD8$^+$ T cells undergo apoptosis, but a heterogeneous population of long-lived memory T cells remain in the circulation and reside in tissues [6, 11, 12]. During many chronic infections, a pool of effector and memory CD8$^+$ T cells will persist that contribute to the long-term control of the pathogen [13-16]. Multiple studies have documented heterogeneity in the phenotype, function, longevity, and fate of these pathogen specific CD8$^+$ T cells [8, 17, 18], but it is unclear whether re-encounter with cognate antigen at local sites of infection contributes to the observed diversity.

In current models, antigen experienced T cells are less dependent on signal 2 and 3, and stimulation through the TCR is considered the critical signal that induces local effector activities [19, 20]. However, previously activated T cells can respond to signals 2 and 3 to mediate effector functions that include the production of cytokines such as IFN-γ [21-23]. The ability to assess T cell function and activation status at sites of infection and inflammation has depended on changes in the expression of surface proteins such as CD69, CD44 and LFA-1, the use of genetically

encoded reporters of cytokine production or the ability to secrete cytokines on re-stimulation, and even intravital imaging of their behavior [24-26]. These approaches have been complimented by protein and transcriptional profiling that have highlighted phenotypic and functional heterogeneity and how functionality and phenotype of $CD8^+$ T cells varies with different pathogens [1, 27, 28]. Nevertheless, certain combinations of surface molecules, such as chemokine receptors as well as activating or inhibitory receptors have helped define different T cell subsets. In certain viral and bacterial infections, the use of graded expression of the chemokine receptor CX3CR1 along with KLRG1 has been used to distinguish effector and memory $CD8^+$ T cell populations [8, 9]. Likewise, during toxoplasmosis, the co-expression of cell surface receptors KLRG1 and CXCR3 distinguishes $CD8^+$ T cell subsets that have memory potential or are terminally differentiated, with continued presence of infection driving the $KLRG1^+CXCR3^-$ terminally differentiated population [18, 29].

As a consequence of T cell activation, changes in the levels of surface markers such as LFA-1, CD44, and CD69 have been useful to identify antigen experienced T cell populations, but it has been a challenge to distinguish those T cell populations that have undergone recent TCR mediated activation [30]. Thus, while TCR signals promote a marked increase in CD69, this transmembrane C type lectin associated with tissue retention is also upregulated by inflammatory signals, its downregulation is varied and following clearance of antigen CD69 is constitutively expressed on Trm populations [31-34]. Genetically encoded reporters of calcium flux have been useful for imaging of TCR signals *in vivo* [24], however these calcium fluxes are rapid and transient and this method does not permit long term tracking or isolation of antigen stimulated cells. Nur77 is an orphan nuclear hormone receptor that is upregulated quickly following stimulation of the TCR [35-38] and transgenic mice that express Nur77-GFP have been used to identify T cells that have experienced recent TCR engagement during priming and the effector phase of T cell responses [35, 36, 39].

Toxoplasma gondii is a ubiquitous obligate intracellular parasite that naturally infects many intermediate hosts, including both humans and mice [40]. Resistance to *T. gondii* is dependent on cell mediated immunity and as a natural host for this pathogen, the mouse has provided a tractable model that helped established the role of IFN-γ and $CD8^+$ T cells in resistance to intracellular infection [14, 18, 41-43]. The early phase of infection is characterized by high levels of replication of the tachyzoite stage of the parasite and vascular dissemination to multiple tissues [44-46]. This phase of infection generates a robust T cell response that restricts parasite growth, but the ability of *T. gondii* to form latent tissue cysts in neurons allows infection to persist in the CNS [43, 47]. However, in patients with acquired defects in T cell responses, the reactivation of the tissue cysts can lead to the development of toxoplasmic encephalitis (TE) [40, 48]. This is recapitulated in mice where long-term control of *T. gondii* is mediated by $CD4^+$ and $CD8^+$ T cell production of IFN-γ which activates a variety of anti-microbial mechanisms in hematopoietic and non-hematopoietic cell types [49-51]. Analysis of the $CD8^+$ T cell responses during acute and chronic toxoplasmosis has highlighted mechanisms that generate and sustain $CD8^+$ T cell responses in the periphery [29, 52-54] as well as the presence of a sub-population of Trm-like cell populations in the CNS [18, 33, 52] that are mirrored in other infections [11, 55].

The ability to modify *T. gondii* to express model antigens such as ovalbumin (OVA), combined with TCR transgenics has provided an important tool to understand T cell responses to this infection [56-60]. This approach allowed the study of early events that lead to parasite specific T cell responses and how these operate in the CNS [18, 61, 62]. Here, OT-I $CD8^+$ T cells specific for the OVA peptide SIINFEKL and expressing Nur77-GFP were combined with *T. gondii*-OVA to identify cells that had recently engaged their TCR and asses how this impacted function. Although TCR activity has been linked to memory formation [63], an adoptive transfer model indicated that during the acute phase recent TCR stimulation did not influence the ability to form long lived memory T cells. During the chronic stage of infection, tachyzoite replication in the CNS was

associated with TCR activation, large scale transcriptional changes, and the acquisition of an effector T cell phenotype as well as the generation of a local population of Trm like cells. However, while inhibition of parasite replication resulted in reduced effector responses it did not alter the Trm population. These data sets highlight the contribution of recent TCR activation on the phenotypic heterogeneity of the $CD8^+$ T cell response but suggest that T cell memory formation and maintenance is independent of recent TCR activation.

Results

Nur77-GFP reporter detects recent T. gondii*-mediated TCR activation*

To track TCR activation in a defined population of $CD8^+$ T cells, transgenic mice were generated that express the OT-I TCR specific for the H2-Kb restricted SIINFKL peptide and the Nur77-GFP reporter (Nur77-GFP OT-I). As expected, naive Nur77-GFP OT-I stimulated with αCD3 *in vitro* induced expression of GFP within 45 minutes that peaked by 2 hours (Figure 1A). Removal of αCD3 stimulation resulted in downregulation of GFP expression within 24-36 hours with basal levels by 72 hours (Figure 1B). This stimulation was accompanied by expression of CD69 which persisted after T cells were rested and had lost GFP expression (Figure 1C). When rested OT-I were restimulated with αCD3 there was rapid re-expression of Nur77-GFP (Figure 1C). The use of peptides with differing affinity for the OT-I TCR revealed a hierarchy wherein a low affinity peptide (EIINFEKL) did not induce reporter expression, moderate affinity peptides (SIIVFEKL and SIIQFEKL) induced intermediate levels of GFP, and the highest levels were associated with SIINFEKL (Supplementary Figure 1A). To test whether Nur77-GFP OT-I encounter with endogenously processed OVA from an infected cell (as opposed to peptide pulsed cells or αCD3) would activate the reporter, bone marrow derived macrophages were infected *in vitro* with a non-replicating strain of *T. gondii* (CPS or CPS-OVA) and co-cultured with naive Nur77-GFP OT-I. With CPS-infected cells there was no induction of GFP and a modest impact on CD69, but co-culture with CPS-OVA infected cells resulted in high levels of GFP and co-expression of CD69 (Figure 1D). To determine if TCR-independent inflammatory signals during infection influence T cell expression of Nur77-GFP, pre-activated and rested Nur77-GFP OT-I T cells were transferred into mice infected with the PRU strain of *T. gondii* or PRU expressing OVA (*T. gondii*-OVA). Although transfer of these T cells into mice infected with *T. gondii* that did not express OVA resulted in a modest increase of CD69, GFP expression was only observed when OT-I were transferred into *T. gondii*-OVA infected mice (Figure 1E). Thus, in the absence of

cognate antigen the inflammatory environment is not sufficient to induce reporter expression. These *in vitro* and *in vivo* data sets validate that the expression of Nur77-GFP provides a sensitive and specific indicator of the recent interaction of OT-I CD8$^+$ T cells with *T. gondii*-derived SIINFEKL.

Infection induced kinetics and phenotype of T. gondii *specific CD8 T cells*

Previous studies have shown infection with *T. gondii*-OVA results in the rapid clonal expansion of OT-I that is dependent on the presence of OVA [28, 56]. To assess the frequency with which these primed T cells re-encounter antigen, 5,000 congenically distinct (CD45.1) naive Nur77-GFP OT-I were transferred into CD45.2 recipients that were then infected with *T. gondii*-OVA that expresses tdTomato. To focus on TCR mediated events after initial priming, mice were analyzed between 10 and 60 days post-infection (dpi). The number of live cells in the spleen that were positive for tdTomato revealed high parasite burden at 10 dpi with a marked decline by days 14 and 20 (Figure 2A). Numbers of OT-I peaked at 14 dpi and the contraction was apparent by 20 dpi (Figure 2B). Mirroring pathogen burden, at 10 dpi GFP$^+$ OT-I in the spleen were readily detected with peak numbers at day 14 (Figure 2B). As parasite burden declined, there was a marked reduction in the numbers and frequency of GFP$^+$ OT-I (Figure 2B).

To determine whether recent TCR stimulation is associated with a distinct phenotype, OT-I were analyzed by high-parameter flow cytometry using markers associated with effector and memory precursor populations (see Materials and Methods for full panel) at 10 dpi. Phenograph clustering indicated that these T cells that had not seen recent TCR appeared as five major clusters, one characterized by the expression of CX3CR1 and CD62L and another associated with reduced expression of activation markers such as CD25 (IL-2Rα) and PD-1 (Figure 2C). In contrast, a majority of GFP$^+$ OT-I were defined by expression of CD25, PD-1, Bim, and Bcl-2, but were low for CX3CR1 and CD62L (Figure 2D, E). Additionally, GFP$^+$ OT-I were more likely to be positive for Ki67 (a marker of entry into cell cycle) and KLRG1 (an inhibitory receptor expressed

by effector T cells) (Figure 2E). Thus, at the peak of the T cell response in the periphery, recent TCR activation is most closely associated with those T cells that express markers of an effector population, but there was a population of effector memory precursor cells ($CX3CR1^{+}KLRG1^{+}$) that appeared less likely to receive TCR signals.

Secondary TCR activation does not impact on ability to form memory

Previous studies have highlighted the impact of TCR activation on the formation of memory populations and the observation that the majority of GFP^{-} OT-I were $KLRG1^{+}$ $CX3CR1^{+}$, whereas the GFP^{+} OT-I were largely $KLRG1^{+}$ $CX3CR1^{-}$ (Figure 3A) suggested that these populations may have different memory potential. To determine if recent antigen stimulation affected the ability to generate memory cell populations, GFP^{-} and GFP^{+} OT-I were sorted from the spleen of day 10 *T. gondii*-OVA infected mice and transferred into naive mice (Figure 3B, C). This process did not lead to infection, based on the absence of $tdTomato^{+}$ cells and lack of GFP expression in the transferred OT-I (Supplementary Figure 2A, B). Nevertheless, 14 days post transfer, OT-I were present in the spleens of these mice but there was no difference in the number of OT-I recovered from the two experimental groups (Figure 3D). In addition, despite differences in the expression of CX3CR1 prior to transfer, the memory cell populations in the mice were all characterized by high expression of CX3CR1 and KLRG1 (Figure 3E), as well as other effector and memory markers such as CXCR3 (Supplementary Figure 2C). These data suggest the population of TCR stimulated cells at day 10 retain the ability to give rise to an effector memory population characterized by co-expression of KLRG1 and CX3CR1.

Influence of TCR stimulation on T cell responses in the CNS

In B6 mice, *T. gondii* enters the CNS as a tachyzoite and foci of parasite replication associated with areas of inflammation are readily apparent. As T cell responses lead to local parasite control, the ability to form tissue cysts (that contain bradyzoites) within neurons allows

198 persistent infection, although periodic reactivation of cysts can lead to areas of tachyzoite
199 replication. Indeed, parasites were detected in the CNS at 10 dpi and the number of tachyzoite
200 infected leukocytes declined between days 20 and 30, although total parasite burden remained
201 high through 40 dpi (Figure 4A). OT-I were recruited to the brain between 10 and 14 dpi (Figure
202 4B) when ~40% of these cells expressed GFP which decreased to ~10-20% of OT-I at 2 months
203 post infection (Figure 4B). The high percentage of GFP^+ cells in the CNS at 10 dpi is at a time
204 point when T cells enter the CNS but infected endothelial cells
205 in the vascular compartment are present [44]. To distinguish the OT-I T cells in the vascular
206 compartment from those that had crossed into the parenchyma of the brain, fluorophore
207 conjugated αCD45 was administered i.v. 3 minutes prior to sacrifice to label vascular resident
208 cells and these populations were compared with those in whole blood. At 10 dpi in the whole
209 blood ~20% of OT-I were GFP^+, with a rapid decline in GFP expression by 14 dpi (Figure 4C)
210 which correlated with the clearance of parasites from circulation. In the CNS at 10 dpi, ~30% of
211 OT-I were vascular and ~40% of these vascular OT-I expressed Nur77-GFP (Figure 4C). By 20
212 dpi, this frequency of brain vascular OT-I had dropped to <5% (Figure 4C) and expression of GFP
213 in these OT-I cells was <20% (Figure4C). At 10 dpi when OT-I are entering the CNS, vascular
214 associated Nur77-GFP+ OT-I were positive for CX3CR1 (Figure 4D), a chemokine receptor
215 involved in T cell trafficking.

216 To determine if there was any differential association in the brain of GFP^+ OT-I with areas
217 of parasite replication, IHC was used to visualize fluorescent parasites, $CD45.1^+$ OT-I T cells, and
218 staining for GFP at day 28. OT-I were widely dispersed throughout the CNS and the majority were
219 Nur77-GFP^-, but Nur77-GFP^+ OT-I were readily observed in association with areas of tachyzoite
220 replication (Figure 4E). In addition, it was noted that a small number of GFP^+ cells were detected
221 in the vicinity of the parasite cyst stage (Figure 4E). Similar results could be detected using live
222 imaging of infected mice, but in which the OT-I did not express the Nur77-GFP reporter, but rather

expressed GFP under the control of the CD4 promoter, as previously described [56]. In this setting, congregation of OT-I around areas of tachyzoite replication, with OT-I that are actively infected by parasite identifiable were readily identified (Supplemental Movie 1). It was also notable that in this OT-I T cells that were non-motile and had a rounded appearance (two behaviors associated with TCR engagement) could be visualized in proximity to a cyst. Together, these data sets highlight that as the infection transitions to the chronic stage in the CNS there are enhanced levels of TCR activation that occurs at the interface between the brain and the vascular system, and in the parenchyma TCR activity appears largely restricted to sites of parasite replication.

Impact of TCR engagement on CD8⁺ T cells during Toxoplasmic Encephalitis

To assess the impact of recent TCR stimulation on the $CD8^+$ T cell population in the CNS, GFP^- and GFP^+ populations of OT-I T cells from the brains of mice infected for 14 days were analyzed by RNA sequencing. Principal component analysis revealed that GFP^- and GFP^+ OT-I formed distinct clusters (Supplementary Figure 3A) and over 2,000 genes were differentially regulated between these populations (adjusted P-value <0.05, logFC >0.3, Figure 5A). In GFP^- OT-I, transcripts for multiple transcription factors associated with memory precursor formation and longevity were upregulated (Figure 5B). The transcriptional profile of GFP^+ OT-I was characteristic of effector T cells and associated with an enrichment of the surface receptors *Cx3cr1* and *Il2ra*, and transcriptional factors (such as *Zeb2* and *Irf8*), as well as those involved in negative regulation of T cell responses (*Egr2* and *Egr3*, Figure 5B). Moreover, an unbiased GSEA analysis revealed the top enriched gene sets of the GFP^+ OT-I were associated with immune cell activation and anti-pathogen responses (Supplementary Figure 3B). As expected, the GFP^+ OT-I were also enriched for gene sets associated with effector functions such as cytotoxicity and IFN-γ production (Figure 5C). This analysis also revealed enrichment of gene sets involved in the negative regulation of TCR mediated signaling (Figure 5C), indicating that an inhibitory feedback loop for TCR signaling was already engaged in those cells.

To determine the differentiation status of GFP$^-$ vs GFP$^+$ OT-I, direct comparison of these subsets with gene signatures derived from LCMV specific CD8$^+$ T cells at different points of infection [1] was performed. This analysis highlighted that GFP$^-$ OT-I had greater abundance of transcripts connected with circulating T cells, as well as signatures associated with late effector CD8$^+$ T cells (Figure 5D). Similar to the GSEA analysis (Figure 5C), the GFP$^+$ OT-I were enriched for early effector molecules and anti-pathogen responses, as well as genes involved in cell division (Figure 5D). Although these T cells express multiple inhibitory receptors such as PD-1, there was no enrichment of a complete set of dysfunction related genes in either the GFP$^-$ or GFP$^+$ OT-I at this time point (Figure 5D). Previous studies have described the presence of a Trm-like population in the CNS during TE [33], and the Trm associated transcripts (*Cpd* and *Adgrg1)* were enriched in GFP$^+$ OT-I, whereas transcripts that are decreased in Trm (*S1pr1* and *Klf2)* had lower abundance in GFP$^+$ OT-I (Figure 5C). Furthermore, when the basal (i.e., not restimulated) ability of OT-I T cells in the brain to produce cytokines was assessed, GFP$^+$ OT-I were 5 times more likely to be producing IFN-γ than GFP$^-$ OT-I (Supplementary Figure 3C). For the OT-I T cells isolated from the brain between 14 and 60 dpi and stimulated with SIINFEKL peptide, the majority of these produced IFN-γ or TNF-α, and degranulated (based on CD107a expression, Figure 5E). These data indicate that TCR activation, rather than bystander activation, is the main stimulus required for effector function during TE and that at these time points there is no overt signature of T cell exhaustion.

Based in part on the transcriptional profiling, high parameter flow cytometry for a panel of markers of activation, memory, exhaustion, and transcription factors was employed to compare the Nur77-GFP OT-I T cell response in the spleen and brain at 2 and 6 weeks post infection. At 14 dpi OT-I phenotypes were distinct between the spleen and brain, with KLRG1 and CX3CR1 co-expression higher in the spleen than brain (Figure 6A). Unsupervised clustering of the brain OT-I at this time point identified 11 unique populations (Figure 6B). There were 7 clusters that

were independent of recent TCR activation, and 4 clusters associated with Nur77-GFP expression (Figure 6B). Clusters that contained the GFP$^+$ OT-I were also enriched for expression of KLRG1, CX3CR1, Tim3, CD25, Ki67 and Bcl-2 (Figure 6C, D). One of the most notable differences is illustrated by the GFP$^+$ OT-I T cell co-expression of KLRG1 and CX3CR1 that are characteristic of effector T cells (Figure 6E).

At 10 dpi, the splenic OT-I were a heterogenous population based on KLRG1 and CX3CR1 (Figure 3A) but by 6 weeks post infection, there was a more homogeneous (>98%) population of OT-I that maintained a KLRG1$^+$CX3CR1$^+$ phenotype (Figure 7A). In contrast, in the brain, the vast majority of OT-I were not positive for CX3CR1 and varied in KLRG1 expression (Figure 7A). In the CNS, segregation by UMAP of the OT-I from 2 and 6 weeks post infection were markedly different phenotypically (Figure 7B). At the 6 week timepoint, approximately 15% of OT-I in the brain were Nur77-GFP$^+$ (Figure 4B). Brain OT-I formed 9 unique clusters (with Nur77-GFP excluded from the UMAP analysis), a subset of GFP$^+$ OT-I clustered differently than GFP$^-$ OT-I by UMAP (Figure 7C). As in the early phase of the T cell response in the brain, KLRG1, Bcl-2, CD25, and Ki67 expression were higher on GFP$^+$ OT-I (Figure 7D, E) and recent TCR activation was still strongly predictive of IFN-γ expression (Figure 7F). These data demonstrate that TCR stimulation contributes to the heterogeneity seen in the CD8$^+$ T cell population, and there is still considerable variation in T cell phenotypes unexplained by recent TCR stimulation.

Impact of parasite replication on TCR on TRM CD8$^+$ T cell phenotype

The transcriptional profiling at day 14 indicated the presence of a Trm signature, consistent with the idea that continued local antigen stimulation may promote or maintain the formation of local Trm cells [64]. Indeed, at 6 weeks post infection, more than 50% of the GFP$^+$ OT-I coexpressed CD69 and CD103, suggesting that recent TCR activation promoted Trm (Figure 8A). To address how antigen levels impact OT-I heterogeneity, *T. gondii*-OVA infected mice were treated with sulfadiazine, a drug that inhibits tachyzoite replication, from days 21 to 49 post

infection, and OT-I were subjected to high dimensional flow cytometry. As expected, based on the detection of tdTomato and PCR, treatment with sulfadiazine reduced parasite burden in the brain (Figure 8B), accompanied by a reduction in the percent of GFP^+ OT-I, as well as the level of reporter expression per cell (Figure 8C). The OT-I isolated from the brains of sulfadiazine treated mice had partial differential clustering on UMAP (Figure 8D), and the most striking impact on this population was the loss of CX3CR1 expression by the GFP^+ OT-I compared to vehicle treated mice (Figure 8E, F). Surprisingly, there was no significant change in the frequency or number of $CD69^+$ $CD103^+$ OT-I in the CNS (Figure 8E, G). These data sets establish that this population of Trm is not dependent on active parasite replication and suggests that antigen may influence Trm phenotype at an earlier stage of activation.

Discussion

Our previous studies have shown that during TE, parasite-specific CD8$^+$ T cells are highly motile and based on their patterns of migration a mathematical model was developed for the ability of these cells to find infected targets [65]. In that report it was unclear what proportion or how frequently the parasite specific CD8$^+$ T cells in the periphery or CNS re-encounter antigen and how this might influence effector function or fate. Here we show that TCR engagement in the periphery and the CNS correlates with levels of infection in these compartments and was as high as ~40% but fell to 10-15% in the chronic stage of infection in the CNS. Given that this Nur77 reporter only provides a snapshot of how many T cells have seen antigen within a narrow time window it appears that the frequency with which CD8$^+$ T cells encounter cognate antigen is high. Similarly, studies utilizing calcium flux reporters in the CNS of mice with high VSV titers concluded that up to 30% of pathogen specific CD8$^+$ T cells were being stimulated by antigen over a short time period [24]. Thus, despite the CNS being a tissue canonically considered immune privileged there are robust levels of antigen presentation and T cell activation that is required for local pathogen control.

While initial TCR stimulation is necessary for T cell priming, few studies have distinguished the role of subsequent antigen exposure on the function and fate of activated effector and memory CD8$^+$ T cells *in vivo*. Many cytokines and transcription factors contribute to the development of T cell heterogeneity, and during toxoplasmosis these include the cytokines IL-7 and IL-12 [66, 67], as well as transcription factors T-bet, c-Rel, BLIMP1, STAT1, and Bhlhe40 [68-73], yet it is unclear whether secondary antigen encounter and TCR activation alters CD8$^+$ T cell fate decisions. The studies presented here show that TCR engagement of activated CD8$^+$ T cells in a secondary site of infection correlated with profound transcriptional changes and expression of markers of effector T cells (for example co-expression of KLRG1 and CX3CR1 and cytokine production). It has been proposed that TCR signal strength and levels of inflammation during priming influence the balance

between effector and memory CD8$^+$ T cells [63, 74]. However, in the transfer studies performed here recent TCR signals did not appear to impact the ability to form a memory CD8$^+$ T cell population. Likewise, the presence of Trm CD8$^+$ T cells in the CNS have been described for other infections [75] and TCR signal strength and duration influences the establishment and function of these Trm populations [76, 77]. A Trm population has also been described during TE [33] and the studies presented here revealed that the OT-I Trm-like cells received frequent TCR stimulation. However, while the absence of active parasite replication resulted in reduced TCR engagement there was no significant change in the frequency or number of these Trm cells in the CNS. Thus, both approaches that addressed the impact of secondary TCR activity on memory populations suggest that recent antigen encounter does not alter these fates and fit with the concept that Trm progenitors are generated early in effector responses [75, 78].

The CNS represents a unique site of inflammation during infection, and the ability of *T. gondii* to establish a persistent infection in this tissue provides the opportunity to study how TCR signals intersect with different phases of the T cell response in the brain. For example, it has been suggested that following challenge with viral or bacterial infections that pathogen replication in the brain is not required for resident CD8$^+$ T cell populations to populate the CNS [79]. However, during toxoplasmosis, endothelial cells of the blood brain barrier are infected [44] and the data that associates CX3CR1 (a chemokine receptor responsible for leukocyte entry into the CNS [80]) with TCR activation in the vascular compartment of the CNS implies that antigen stimulation at the blood brain barrier may induce T cell extravasation into the parenchyma. The use of the Nur77-GFP reporter as a surrogate for TCR activation should provide a sensitive system to assess the host factors that contribute to compartment (vascular, endothelial, and parenchymal) specific T cell activity in the CNS required for T cell mediated protective immunity.

In certain cancers and infection, one of the effects of repetitive antigen stimulation on CD8$^+$ T cells is the induction of T cell exhaustion, denoted by an increase in inhibitory receptors and a

decrease in cytokine secretion and cytolytic capacity [81-83]. During TE, parasite-specific T cells express high levels of inhibitory receptors such as PD-1 and TIGIT and it has been suggested that these T cell populations may be exhausted [82-85]. Indeed, there is a report that PD-L1 blockade leads to enhanced $CD8^+$ T cell responses during TE [83], whereas in a similar setting the absence of TIGIT does not augment the T cell response [84]. The impact of inhibitory receptors during TE is complicated by evidence that PD-1 supports the generation of Trm in the CNS in viral infections [86-88]. Nonetheless, in our studies IFN-γ expression was closely correlated with expression of Nur77-GFP, indicating that TCR-independent bystander cytokine-mediated activation of CD8+ T cells [89-91] is not a major contributor to the production of IFN-γ. Moreover, the functional and transcriptional analysis did not reveal any early signs of exhaustion in Nur77-GFP^+ OT-I. Indeed, the magnitude of differentially expressed genes associated with TCR activation in the CNS was similar in scope to the transcriptional changes observed during priming of OT-I T cells in other models [1]. Many of these upregulated genes were transcription factors and regulators (*Irf8, Batf3, Bach2, Egr2*) known to direct $CD8^+$ T cell function, indicating that subsequent antigen encounter may restructure transcriptional programs. These results also revealed six clusters that were not segregated by Nur77-GFP expression and underscore the need for additional studies to distinguish how priming affects diversity versus the TCR-independent signals that affect the evolution of the T cell response during TE.

There are several neurotropic infections that have distinct developmental states associated with latency and for *T. gondii* this is exemplified by the ability to form the tissue cyst. It has been proposed that the presence of this stage in neurons, a cell type known for low MHC-I expression [92], would be sequestered by the immune response. The idea that neurons can act as a refuge has been challenged by evidence that MHC-I presentation of tachyzoite antigens by neurons contributes to parasite control [58]. Imaging of brains from mice chronically infected with *T. gondii* had higher numbers of Nur77-GFP^+ OT-I surrounding tachyzoites but as the infection in the brain progresses the decline in levels of TCR engagement correlated with parasite control

and the switch from tachyzoite to bradyzoite. However, there were examples where Nur77-GFP$^+$ OT-I were in close proximity to intact cysts but whether this is due to presentation by infected neurons, other glial populations, or infiltrating DC or monocyte populations that interact with infected neurons [56] is currently unknown. Whether the cyst stage is under direct immune surveillance is also unclear but the ability of bradyzoites to actively block IFN-γ signaling [47] implies the need for the parasite to evade an active response against the cyst stage [43, 93]. Currently, there is a paucity of host and parasite specific tools to dissect the ability of host cells to process and present antigens from the bradyzoite life-stage. Future experiments utilizing bradyzoite-specific secretion of model antigens combined with the Nur77-GFP reporter will be utilized to address this knowledge gap.

Materials and Methods

Mice and infection

Nur77-GFP reporter mice, C57BL/6 mice, CD45.1 C57BL/6 mice, and OT-I mice were purchased from Jackson Laboratories. DPE-GFP transgenic mice were originally obtained from Ulrich H. von Andrian (CBR, Harvard, Boston MA) and were crossed to OT-I mice. All mice were housed in a specific-pathogen free environment at the University of Pennsylvania School of Veterinary Medicine in accordance with federal guidelines and with approval of the Institutional Animal Care and Use Committee. The generation of CPS-OVA parasites and PRU-OVA parasites were described previously [28, 59].

Parasites were cultured and maintained by serial passage on human foreskin fibroblast cells in the presence of parasite culture media (DMEM, 20% medium M199, 10% fetal bovine serum (FBS), 1% penicillin-streptomycin, 25 µg/ml gentamycin) which was supplemented with uracil for culturing CPS strain parasites (final concentration of 0.2 mM uracil). Tachyzoites of each strain were prepared for infection by serial 26g needle passage and filtered through a 5-µm-pore-size filter. 1 day prior to infection, 5,000 congenically distinct naive splenic Nur77-GFP OT-I were transferred i.v. into naive mice. Mice were infected i.p. with 10^4 live parasites. In indicated experiments, mice were treated with 250mg/L of sulfadiazine in drinking water for 4 weeks beginning at 3 weeks post infection.

For adoptive transfers of OT-I from infected mice to naive mice, OT-I were double sorted on a BD FACS Aria. Each naive mice received an i.v. transfer of 150,000 Nur77-GFP$^-$ or Nur77-GFP$^+$ pooled from 2 infected mice. Recipient mice were treated with sulfadiazine two days prior and 1 week following transfer to ensure *T. gondii* infection was not transferred.

Parasite quantification by PCR

Approximately 10mg of tissue was snap frozen and DNA was extracted with Qiagen DNeasy Blood and Tissue Kit according to manufacturer's protocol. Real-time PCR was conducted with SYBR Green master mix according to manufacturer's protocol, with 500ng of template DNA. *T. gondii* DNA was amplified with forward (5'-TCCCCTCTGCTGGCGAAAAGT-3') and reverse (5'-AGCGTTCGTGGTCAACTATCGATTG-3') primers to the B1 gene. PCR was performed on an Applied Biosystems ViiA7 with the following cycle conditions: Hold phase: 2min 50C, 10min 95C; PCR phase (occurs 50x): 15s at 95C, 1min @60C.

Tissue processing

Spleens were grinded through a 70uM filter and red blood cells lysed with ACK lysis buffer. Brains were chopped into 1mm sections and incubated at 37C for 1.5 hours with 250ug/mL Collagenase/Dispase and 10ug/mL DNase, passed through a 70uM filter, then leukocytes were isolated through 30% and 60% Percoll density centrifugation.

Quantification of T cell cytokine production

$1x10^6$ brain mononuclear cells were cultured *ex vivo* at 37C for 4 hours in RPMI supplemented with 10% FBS. For restimulations, 1uM of peptide was added with Protein Transport Inhibitor Cocktail. For quantification of endogenous levels of cytokine production, only Protein Transport Inhibitor Cocktail was added.

Bone marrow macrophage culture

Bone marrow macrophages were isolated and cultured for 7 days with 30% L929 media in DMEM with 10% FBS, with media replenishing on day 4 after isolation. For peptide stimulations, 1uM of peptide was added to macrophages for 20 minutes and excess peptide was removed by washing 2 times. For parasite infection, a parasite to macrophage infection ratio of 2:1 was used, and excess parasites were removed by washing 2 times. $CD8^+$ T cell were isolated by MACS bead enrichment. Macrophages and T cells were cultured at a 1:2 ratio.

Flow cytometry

Staining of extracellular antigens was performed following Fc receptor blocking with Rat IgG and anti-mouse CD16/CD32. Intracellular antigens were stained following fixation and permeabilization using the Foxp3 Transcription Factor Staining Buffer Set. All samples were run on a BD FACSymphony A5 or BD FACSCanto and analyzed on FlowJo v10 software (FlowJo, Ashland, OR). UMAP and Phenograph were utilized in FlowJo for dimensionality reduction and unsupervised clustering.

Imaging

Brains were fixed in 4% paraformaldehyde overnight, followed by 15% and 30% sucrose in PBS overnight. 12uM sections were stained with AF488 anti-GFP and AF647 anti-CD45.1 in 0.1% Triton-X100 and 0.05% Tween-20 in PBS. Slides were sealed with Prolong Diamond Antifade Mountant with DAPI. Slides were imaged at 60x magnification on a Leica SP5-II (Lecia, Wetzlar, Germany).

Live imaging of brain explants was performed as previously described [65]. Briefly, mice were infected with PRU-OVA parasites expressing tdTomato. Four weeks following infection, mice received $2x10^6$ activated DPE-GFP-OT-I i.v., and brains were imaged one week following transfer of DPE-GFP-OT-I. Imaging was performed on an Lecia SP5 multiphoton.

RNA sequencing

Nur77-GFP- and Nur77-GFP+ OT-I were double sorted as described above. Cells were collected in RPMI with 20% FBS and resuspended in Buffer RLT Plus. mRNA was isolated using RNeasy Micro Plus Kit and RNA quality was evaluated by High Sensitivity RNA Screen Tape on an Agilent 4200 TapeStation. cDNA library was prepared with Takara SMART-Seq HT kit and adapters ligated with Nextera XT DNA Library Preparation Kit and Index Kit v2 according to manufacturers' protocols. AMPure XP beads were used for primer cleanup. 75-base pair reads were sequenced

on a NextSeq 500 machine (Illumina, San Diego, CA)) according to manufacturer protocol. Kallisto was utilized to pseudo-align genes to version 75 of the mouse reference genome GRCm38. Transcripts that were represented in fewer than 3 of 4 samples in a group were excluded from analysis. The limma package in R was used to generate normalized counts per million, and differential genes (adjusted P-value>0.05) were identified with a log fold change cutoff of 0.3. The heatmaply package was used for heatmap generation. Gene set enrichment analysis was performed with GSEA software (v4.0.3, Broad Institute) with gene sets containing less than 10 genes excluded. Enrichment plots were generated in Cytoscape (v3.7.1) with an adjusted P-value cutoff of 0.05 and false discovery rate cutoff of 0.1 (pipeline adapted from [94]). Data is deposited in GEO (accession# GSE188495).

Fluorophore	**Target**	**Clone**	**Catalog #**	**Source**
BUV395	KLRG1	2F1	740279	Becton Dickinson (Franklin Lakes, NJ)
BUV563	CD8a	53-6.7	748535	Becton Dickinson
BUV615	Va2	B20.1	751416	Becton Dickinson
BUV661	IL2Rb	TM-β1	741493	Becton Dickinson
BUV737	CD69	H1.2F3	612793	Becton Dickinson
BUV805	CD11a	2D7	741919	Becton Dickinson
BV421	PD-1	29F.1A12	135218	BioLegend (San Diego, CA)
AQUA	Viability		13-0870	Tonbo Biosciences (San Diego, CA)
BV570	Ly6c	HK1.4	128030	BioLegend
BV605	CD103	2E7	121433	BioLegend
BV650	CD25	PC61	102038	BioLegend
BV711	CD45.1	A20	110739	BioLegend
BV785	CX3CR1	SA011F11	149029	BioLegend
APCef780	CD62L	MEL-14	47-0621-82	eBioscience (San Diego, CA)
PE	Tim3	134004	B8.2C12	BioLegend
PECy7	CD127	A7R34	135014	BioLegend
Unconjugated	BIM	K.912.7	MA5-14848	Invitrogen (Waltham, MA)
AF350	goat anti-rabbit	Polyclonal	A-11046	Invitrogen

AF488	GFP	FM264G	338008	BioLegend
BV480	Ki67	B56	566109	Becton Dickinson
AF647	Bcl2	BCL/10C4	633510	BioLegend
PECY5	Tbet	4B10	15-5825-82	eBioscience
AF700	CD45	30-F11	103128	BioLegend
PECy7	CD107a	1D4B	121620	BioLegend
AF647	CD45.1	A20	110720	BioLegend
APC	IFN-γ	XMG1.2	17-7311-82	Invitrogen
BV711	TNFα	MP6-XT22	506349	BioLegend
PECy7	CD8b	53-5.8	140416	BioLegend

475

Reagent	**Source**	**Catalog #**
C57Bl/6 Mice	Jackson Laboratories	000664
CD45.1 C57Bl/6 Mice	Jackson Laboratories	002014
Nur77-GFP Mice	Jackson Laboratories	016617
OT-I Mice	Jackson Laboratories	003831
DNeasy Blood and Tissue Kit	Qiagen	69506
ProLong Diamond Antifade Mountant with DAPI	Invitrogen	P36962
SIINFEKL peptide	Biosyn	Custom
SIIVFEKL peptide	Biosyn	Custom
SIIQFEKL peptide	Biosyn	Custom
EIINFEKL peptide	Biosyn	Custom
Protein Transport Inhibitor Cocktail	eBioscience	00-4980-93
DMEM Media	Corning	15017CV
M199 Media	Gibco	11150059
RPMI	Corning	10041CM
Fetal Bovine Serum	Sigma-Aldrich	F0926
Penicillin-Streptomycin	Gibco	15140122
Gentamycin	Gibco	15710064
Sulfadiazine	Sigma-Aldrich	S8626
SYBR Green Master Mix	Applied Biosystems	4309155
Collagenase/Dispase	Roche	10269638001
Dnase I	Roche	10104159001
Percoll	GE Healthcare	17-0891-01
CD8+ T Cell Isolation Kit, mouse	Miltenyi Biotec	130-104-075
Paraformaldehyde	ProSciTech	15710-S
Sucrose	Sigma-Aldrich	57-50-1
Triton-X100	ThermoFisher	28313
Tween-20	Sigma-Aldrich	P1379
Buffer RLT Plus	Qiagen	1053393

RNeasy Micro Plus Kit	Qiagen	74034
High Sensitivity RNA ScreenTape	Agilent	5067-5579
High Sensitivity RNA Ladder	Agilent	5067-5581
High Sensitivity RNA Buffer	Agilent	5067-5580
AMPure XP beads	Beckman Coulter	A63881
Foxp3 / Transcription Factor Staining Buffer Set	eBioscience	00-5523-00

476

Figure Legends

Fig 1. Nur77-GFP OT-I respond to *T. gondii* antigen.

(A-B) Naive OT-I stimulated *in vitro* with plate bound αCD3 and αCD28 for up to 48 hours, then removed from stimulation. (C) Rested OT-I restimulated with αCD3. (D) BMDM infected with CPS or CPS-OVA and co-cultured with OT-I. (E) Splenic OT-I following infection with *T. gondii* or *T. gondii*-OVA (N=3 mice per group). P values based on Students T-test with Bonferroni-Dunn correction for multiple comparisons; error bars indicate SEM.

Fig 2. Infection induced kinetics and phenotype of splenic *T. gondii* specific CD8$^+$ T cells.

(A-B) OT-I were transferred i.v. into naive mice and infected with *T. gondii*-OVA. Mice were sacrificed between 10 and 60 dpi and spleens were analyzed (N=4-6 mice per time point). (C-E) High dimensional flow cytometry with UMAP and Phenograph clustering was performed on splenic OT-I at 10 dpi. P values based on Paired T-test; error bars indicate SEM.

Fig 3. CD8$^+$ T cell memory potential retained in Nur77-GFP$^+$ OT-I.

(A) OT-I from spleen of *T. gondii*-OVA 10 dpi. (B-C) OT-I from spleen of T. gondii-OVA 10 dpi were sorted by Nur77-GFP expression and transferred into naive mice. Mice were sacrificed 14 days post transfer (N=4 mice). (D) Identification of OT-I from mice receiving either Nur77-GFP$^+$ or Nur77-GFP$^-$ OT-I. (E-F) Characterization of OT-I from recipient mice. P values based on Students T-test with Bonferroni-Dunn correction for multiple comparisons; error bars indicate SEM.

Fig 4. Infection induced kinetics of CNS *T. gondii* specific CD8$^+$ T cells.

(A-B) Kinetics of infection and OT-I in the brain following infection with *T. gondii*-OVA (N=4-6 mice per time point). (C) Mice were given i.v. dose of fluorophore conjugated αCD45 prior to sacrifice to label vascular cells. OT-I from whole blood were compared to OT-I from the vascular labeled

fraction of the brain. P values based on Two-Way ANOVA; error bars indicate SEM. (D) Nur77-GFP+ OT-I from the CNS of *T. gondii*-OVA infected mice at 10 dpi. (E) Brain sections were stained for CD45.1 (white) to identify OT-I, anti-GFP (green) to identify recently TCR stimulated OT-I, DAPI (blue) to identify nuclei, and were infected with *T. gondii*-OVA expressing tdTomato (red). Number of Nur77-GFP+ OT-I surrounding parasites were counted. Arrows indicate Nur77-GFP$^+$ OT-I. (F) *Ex vivo* imaging of constitutive GFP expressing OT-I (green) in brain explants of *T. gondii*-OVA (red) infected mice. Arrows indicate *T. gondii* infection. P values based on Students T-test; error bars indicate SEM.

Fig 5. Transcriptional profiling of Nur77-GFP OT-I from CNS.

(A-D) Nur77-GFP$^-$ and Nur77-GFP$^+$ OT-I from the brains of mice infected with *T. gondii*-OVA 14 dpi were transcriptionally profiled using RNA-sequencing. (A) Volcano plot of all transcripts. Lines indicate logFC > 0.03 and adjusted P-value > 0.05. (B) Heatmap of differentially expressed genes involved in CD8+ T cell activation, differentiation, memory formation, and effector function. (C) Top GSEA enriched pathways in Nur77-GFP$^+$ OT-I compared to Nur77-GFP$^-$ OT-I. (D) Gene sets involved in CD8+ T cell activation and differentiation (red dots). (E) OT-I from brains of *T. gondii*-OVA infected mice were restimulated with SIINFEKL peptide and cytokine and degranulation was assessed by flow cytometry.

Fig 6. Infection induced phenotype of CNS *T. gondii* specific CD8$^+$ T cells during early infection.

(A) Phenotype of OT-I in spleen and brain of *T. gondii*-OVA infected mice 14 dpi. (B-E) High dimensional flow cytometry with UMAP and Phenograph clustering was performed on brain OT-I at 14 dpi. P values based on Paired T-test; error bars indicate SEM.

Fig 7. Infection induced phenotype and function of CNS *T. gondii* specific CD8$^+$ T cells during chronic infection.

(A) High dimensional flow cytometry with UMAP of OT-I from brains of mice infected with *T. gondii*-OVA at 14 dpi and 6 weeks post infection. (B) Phenotype of OT-I in spleen and brain of *T. gondii*-OVA infected mice 6 weeks post infection. (C-E) High dimensional flow cytometry with UMAP and Phenograph clustering was performed on brain OT-I at 6 weeks post infection. (F) Endogenous levels of IFN-γ expression in Nur77-GFP- and Nur77-GFP+ OT-I following 4-hour culture with protein transport inhibitor. P values based on Paired T-test; error bars indicate SEM.

Fig 8. Impact of parasite replication of CNS CD8⁺ T cell phenotype.

(A) Trm phenotype of OT-I at 6 weeks post infection in the brain. P values based on Paired T-test; error bars indicate SEM. (B-G) *T. gondii*-OVA infected mice were treated with sulfadiazine from 3 weeks to 7 weeks post infection and parasite burden and OT-I phenotype was assessed at 7 weeks. P values based on Students T-test (B-C) or Two-Way ANOVA (F); error bars indicate SEM.

Supplemental Movie 1. *Ex vivo* imaging of OT-I in the CNS of *T. gondii* infected mice.

Behavior of constitutive GFP OT-I T cells (green) in the brains of mice infected with *T. gondii*-OVA (red). OT-I were transferred into chronically infected mice and imaged one week post transfer. Live imaging of brain explants.

Supplementary Fig 1. Effect of TCR signal strength on Nur77-GFP OT-I reporter activity.

(A) Peptide pulsed splenocytes were incubated with Nur77-GFP OT-I and reporter activity was assessed at 3 hours.

Supplementary Fig 2. Transfer of Nur77-GFP OT-I from *T. gondii* infected mice into naive mice.

Lack of infection at 14 days post transfer measured by (A) tdTomato expression of total splenocytes or (B) Nur77-GFP expression in transferred OT-I. (C) KLRG1 and CXCR3 expression

of Nur77-GFP- and Nur77-GFP+ OT-I prior to transfer at 10 dpi and 14 days post transfer. P values based on Two-Way ANOVA; error bars indicate SEM.

Supplementary Fig 3. Transcriptional profiling of Nur77-GFP OT-I from CNS.

(A) PCA plot of Nur77-GFP$^-$ and Nur77-GFP$^+$ OT-I. (B) Top GSEA gene sets with FDR>0.05 enriched in Nur77-GFP$^+$ OT-I compared to Nur77-GFP$^-$ OT-I. (C) Endogenous cytokine production of Nur77-GFP$^-$ and Nur77-GFP$^+$ OT-I from the CNS of *T. gondii*-OVA infected mice at 14 dpi.

554 **References**

555 1. Best JA, Blair DA, Knell J, Yang E, Mayya V, Doedens A, Dustin ML, Goldrath AW,
556 Immunological Genome Project C. Transcriptional insights into the CD8(+) T cell response to
557 infection and memory T cell formation. Nat Immunol. 2013;14(4):404-12. Epub 2013/02/12. doi:
558 10.1038/ni.2536. PubMed PMID: 23396170; PubMed Central PMCID: PMCPMC3689652.
559 2. Wakim LM, Woodward-Davis A, Bevan MJ. Memory T cells persisting within the brain after
560 local infection show functional adaptations to their tissue of residence. Proc Natl Acad Sci U S A.
561 2010;107(42):17872-9. Epub 2010/10/07. doi: 10.1073/pnas.1010201107. PubMed PMID:
562 20923878; PubMed Central PMCID: PMCPMC2964240.
563 3. Wakim LM, Woodward-Davis A, Liu R, Hu Y, Villadangos J, Smyth G, Bevan MJ. The
564 molecular signature of tissue resident memory CD8 T cells isolated from the brain. J Immunol.
565 2012;189(7):3462-71. Epub 2012/08/28. doi: 10.4049/jimmunol.1201305. PubMed PMID:
566 22922816; PubMed Central PMCID: PMCPMC3884813.
567 4. Henrickson SE, Perro M, Loughhead SM, Senman B, Stutte S, Quigley M, Alexe G,
568 Iannacone M, Flynn MP, Omid S, Jesneck JL, Imam S, Mempel TR, Mazo IB, Haining WN, von
569 Andrian UH. Antigen availability determines CD8(+) T cell-dendritic cell interaction kinetics and
570 memory fate decisions. Immunity. 2013;39(3):496-507. Epub 2013/09/24. doi:
571 10.1016/j.immuni.2013.08.034. PubMed PMID: 24054328; PubMed Central PMCID:
572 PMCPMC3914670.
573 5. Butz EA BM. Massive Expansion of Antigen-Specific CD8+ T Cells during an Acute Virus
574 Infection. Immunity. 1998;8(2):167-75. doi: 10.1016/s1074-7613(00)80469-0.
575 6. Jameson SC, Masopust D. Understanding Subset Diversity in T Cell Memory. Immunity.
576 2018;48(2):214-26. Epub 2018/02/22. doi: 10.1016/j.immuni.2018.02.010. PubMed PMID:
577 29466754; PubMed Central PMCID: PMCPMC5863745.

578 7. Bottcher JP, Beyer M, Meissner F, Abdullah Z, Sander J, Hochst B, Eickhoff S, Rieckmann
579 JC, Russo C, Bauer T, Flecken T, Giesen D, Engel D, Jung S, Busch DH, Protzer U, Thimme R,
580 Mann M, Kurts C, Schultze JL, Kastenmuller W, Knolle PA. Functional classification of memory
581 CD8(+) T cells by CX3CR1 expression. Nat Commun. 2015;6:8306. Epub 2015/09/26. doi:
582 10.1038/ncomms9306. PubMed PMID: 26404698; PubMed Central PMCID: PMCPMC4667439.
583 8. Gerlach C, Moseman EA, Loughhead SM, Alvarez D, Zwijnenburg AJ, Waanders L, Garg
584 R, de la Torre JC, von Andrian UH. The Chemokine Receptor CX3CR1 Defines Three Antigen-
585 Experienced CD8 T Cell Subsets with Distinct Roles in Immune Surveillance and Homeostasis.
586 Immunity. 2016;45(6):1270-84. Epub 2016/12/13. doi: 10.1016/j.immuni.2016.10.018. PubMed
587 PMID: 27939671; PubMed Central PMCID: PMCPMC5177508.
588 9. Herndler-Brandstetter D, Ishigame H, Shinnakasu R, Plajer V, Stecher C, Zhao J,
589 Lietzenmayer M, Kroehling L, Takumi A, Kometani K, Inoue T, Kluger Y, Kaech SM, Kurosaki T,
590 Okada T, Flavell RA. KLRG1(+) Effector CD8(+) T Cells Lose KLRG1, Differentiate into All
591 Memory T Cell Lineages, and Convey Enhanced Protective Immunity. Immunity. 2018;48(4):716-
592 29 e8. Epub 2018/04/08. doi: 10.1016/j.immuni.2018.03.015. PubMed PMID: 29625895; PubMed
593 Central PMCID: PMCPMC6465538.
594 10. Badovinac VP, Haring JS, Harty JT. Initial T cell receptor transgenic cell precursor
595 frequency dictates critical aspects of the CD8(+) T cell response to infection. Immunity.
596 2007;26(6):827-41. Epub 2007/06/09. doi: 10.1016/j.immuni.2007.04.013. PubMed PMID:
597 17555991; PubMed Central PMCID: PMCPMC1989155.
598 11. Badovinac VP, Porter BB, Harty JT. Programmed contraction of CD8(+) T cells after
599 infection. Nat Immunol. 2002;3(7):619-26. Epub 2002/06/11. doi: 10.1038/ni804. PubMed PMID:
600 12055624.
601 12. Bachmann MF, Wolint P, Schwarz K, Jager P, Oxenius A. Functional properties and
602 lineage relationship of CD8+ T cell subsets identified by expression of IL-7 receptor alpha and

603 CD62L. J Immunol. 2005;175(7):4686-96. Epub 2005/09/24. doi: 10.4049/jimmunol.175.7.4686.
604 PubMed PMID: 16177116.
605 13. Jin X BD, Tuttleton SE, Lewin S, Gettie A, Blanchard J, Irwin CE, Safrit JT, Mittler J,
606 Weinberger L, Kostrikis LG, Zhang L, Perelson AS, Ho DD. Dramatic rise in plasma viremia after
607 CD8(+) T cell depletion in simian immunodeficiency virus-infected macaques. J Exp Med.
608 189(6):991-8. doi: 10.1084/jem.189.6.991.
609 14. Suzuki Y RJ. Dual regulation of resistance against Toxoplasma gondii infection by Lyt-2+
610 and Lyt-1+, L3T4+ T cells in mice. J Immunol. 1988;140(11):3943-6.
611 15. Fröhlich A, Kisielow J, Schmitz I, Freigang S, Shamshiev AT, Weber J, Marsland BJ,
612 Oxenius A, Kopf M. IL-21R on T Cells Is Critical for Sustained Functionality and Control of Chronic
613 Viral Infection. Science. 2009;324(5934):1576-80. doi: doi:10.1126/science.1172815.
614 16. Paley MA, Kroy DC, Odorizzi PM, Johnnidis JB, Dolfi DV, Barnett BE, Bikoff EK,
615 Robertson EJ, Lauer GM, Reiner SL, Wherry EJ. Progenitor and Terminal Subsets of CD8+ T
616 Cells Cooperate to Contain Chronic Viral Infection. Science. 2012;338(6111):1220-5. doi:
617 doi:10.1126/science.1229620.
618 17. Gerlach C RJ, Perié L, van Rooij N, van Heijst JW, Velds A, Urbanus J, Naik SH, Jacobs
619 H, Beltman JB, de Boer RJ, Schumacher TN. Heterogeneous differentiation patterns of individual
620 CD8+ T cells. Science. 2014;340:635-9. doi: 10.1126/science.1235487.
621 18. Chu HH, Chan SW, Gosling JP, Blanchard N, Tsitsiklis A, Lythe G, Shastri N, Molina-Paris
622 C, Robey EA. Continuous Effector CD8(+) T Cell Production in a Controlled Persistent Infection
623 Is Sustained by a Proliferative Intermediate Population. Immunity. 2016;45(1):159-71. Epub
624 2016/07/17. doi: 10.1016/j.immuni.2016.06.013. PubMed PMID: 27421704; PubMed Central
625 PMCID: PMCPMC4956557.
626 19. Suresh M, Whitmire JK, Harrington LE, Larsen CP, Pearson TC, Altman JD, Ahmed R.
627 Role of CD28-B7 interactions in generation and maintenance of CD8 T cell memory. J Immunol.

628 2001;167(10):5565-73. Epub 2001/11/08. doi: 10.4049/jimmunol.167.10.5565. PubMed PMID:
629 11698427.
630 20. Byers AM, Kemball CC, Moser JM, Lukacher AE. Cutting edge: rapid in vivo CTL activity
631 by polyoma virus-specific effector and memory CD8+ T cells. J Immunol. 2003;171(1):17-21.
632 Epub 2003/06/21. doi: 10.4049/jimmunol.171.1.17. PubMed PMID: 12816977.
633 21. Murphy EE TG, Macatonia SE, Hsieh CS, Mattson J, Lanier L, Wysocka M, Trinchieri G,
634 Murphy K, O'Garra A. B7 and interleukin 12 cooperate for proliferation and interferon gamma
635 production by mouse T helper clones that are unresponsive to B7 costimulation. J Exp Med.
636 1994;180(1):223-31. doi: 10.1084/jem.180.1.223.
637 22. Lertmemongkolchai G, Cai G, Hunter CA, Bancroft GJ. Bystander activation of CD8+ T
638 cells contributes to the rapid production of IFN-gamma in response to bacterial pathogens. J
639 Immunol. 2001;166(2):1097-105. Epub 2001/01/06. doi: 10.4049/jimmunol.166.2.1097. PubMed
640 PMID: 11145690.
641 23. Yang J MT, Ouyang W, Murphy KM. Induction of interferon-gamma production in Th1
642 CD4+ T cells: evidence for two distinct pathways for promoter activation. Eur J Immunol.
643 1999;29(2):548-55.
644 24. Moseman EA BA, Nayak D, McGavern DB. T cell engagement of cross-presenting
645 microglia protects the brain from a nasal virus infection. Science Immunology. 2020;8(48). doi:
646 10.1126/sciimmunol.abb1817.
647 25. Baaten BJ, Tinoco R, Chen AT, Bradley LM. Regulation of Antigen-Experienced T Cells:
648 Lessons from the Quintessential Memory Marker CD44. Front Immunol. 2012;3:23. Epub
649 2012/05/09. doi: 10.3389/fimmu.2012.00023. PubMed PMID: 22566907; PubMed Central
650 PMCID: PMCPMC3342067.
651 26. Reinhardt RL, Liang HE, Locksley RM. Cytokine-secreting follicular T cells shape the
652 antibody repertoire. Nat Immunol. 2009;10(4):385-93. Epub 2009/03/03. doi: 10.1038/ni.1715.
653 PubMed PMID: 19252490; PubMed Central PMCID: PMCPMC2714053.

654 27. Kiner E, Willie E, Vijaykumar B, Chowdhary K, Schmutz H, Chandler J, Schnell A, Thakore
655 PI, LeGros G, Mostafavi S, Mathis D, Benoist C, Immunological Genome Project C. Gut CD4(+)
656 T cell phenotypes are a continuum molded by microbes, not by TH archetypes. Nat Immunol.
657 2021;22(2):216-28. Epub 2021/01/20. doi: 10.1038/s41590-020-00836-7. PubMed PMID:
658 33462454; PubMed Central PMCID: PMCPMC7839314.
659 28. Jordan KA, Wilson EH, Tait ED, Fox BA, Roos DS, Bzik DJ, Dzierszinski F, Hunter CA.
660 Kinetics and phenotype of vaccine-induced CD8+ T-cell responses to Toxoplasma gondii. Infect
661 Immun. 2009;77(9):3894-901. Epub 2009/06/17. doi: 10.1128/IAI.00024-09. PubMed PMID:
662 19528214; PubMed Central PMCID: PMCPMC2738025.
663 29. Shah S, Grotenbreg GM, Rivera A, Yap GS. An extrafollicular pathway for the generation
664 of effector CD8(+) T cells driven by the proinflammatory cytokine, IL-12. Elife. 2015;4. Epub
665 2015/08/06. doi: 10.7554/eLife.09017. PubMed PMID: 26244629; PubMed Central PMCID:
666 PMCPMC4549662.
667 30. Warnock RA AS, Butcher EC, von Andrian UH. Molecular mechanisms of lymphocyte
668 homing to peripheral lymph nodes. J Exp Med. 1998;187(2):205-16. doi: 10.1084/jem.187.2.205.
669 31. Masopust D, Vezys V, Usherwood EJ, Cauley LS, Olson S, Marzo AL, Ward RL,
670 Woodland DL, Lefrancois L. Activated primary and memory CD8 T cells migrate to nonlymphoid
671 tissues regardless of site of activation or tissue of origin. J Immunol. 2004;172(8):4875-82. Epub
672 2004/04/07. doi: 10.4049/jimmunol.172.8.4875. PubMed PMID: 15067066.
673 32. Ariotti S, Haanen JB, Schumacher TN. Behavior and function of tissue-resident memory
674 T cells. Adv Immunol. 2012;114:203-16. Epub 2012/03/28. doi: 10.1016/B978-0-12-396548-
675 6.00008-1. PubMed PMID: 22449783.
676 33. Landrith TA, Sureshchandra S, Rivera A, Jang JC, Rais M, Nair MG, Messaoudi I, Wilson
677 EH. CD103(+) CD8 T Cells in the Toxoplasma-Infected Brain Exhibit a Tissue-Resident Memory
678 Transcriptional Profile. Front Immunol. 2017;8:335. Epub 2017/04/21. doi:

679 10.3389/fimmu.2017.00335. PubMed PMID: 28424687; PubMed Central PMCID:
680 PMCPMC5372813.
681 34. Mackay LK, Rahimpour A, Ma JZ, Collins N, Stock AT, Hafon ML, Vega-Ramos J,
682 Lauzurica P, Mueller SN, Stefanovic T, Tscharke DC, Heath WR, Inouye M, Carbone FR,
683 Gebhardt T. The developmental pathway for CD103(+)CD8+ tissue-resident memory T cells of
684 skin. Nat Immunol. 2013;14(12):1294-301. Epub 2013/10/29. doi: 10.1038/ni.2744. PubMed
685 PMID: 24162776.
686 35. Moran AE, Holzapfel KL, Xing Y, Cunningham NR, Maltzman JS, Punt J, Hogquist KA. T
687 cell receptor signal strength in Treg and iNKT cell development demonstrated by a novel
688 fluorescent reporter mouse. J Exp Med. 2011;208(6):1279-89. Epub 2011/05/25. doi:
689 10.1084/jem.20110308. PubMed PMID: 21606508; PubMed Central PMCID: PMCPMC3173240.
690 36. Low JS, Farsakoglu Y, Amezcua Vesely MC, Sefik E, Kelly JB, Harman CCD, Jackson R,
691 Shyer JA, Jiang X, Cauley LS, Flavell RA, Kaech SM. Tissue-resident memory T cell reactivation
692 by diverse antigen-presenting cells imparts distinct functional responses. J Exp Med. 2020;217(8).
693 Epub 2020/06/12. doi: 10.1084/jem.20192291. PubMed PMID: 32525985; PubMed Central
694 PMCID: PMCPMC7398161 personal fees from the JEM Editorial Board outside the submitted
695 work. No other disclosures were reported.
696 37. Ashouri JF, Weiss A. Endogenous Nur77 Is a Specific Indicator of Antigen Receptor
697 Signaling in Human T and B Cells. J Immunol. 2017;198(2):657-68. Epub 2016/12/13. doi:
698 10.4049/jimmunol.1601301. PubMed PMID: 27940659; PubMed Central PMCID:
699 PMCPMC5224971.
700 38. Zemmour D, Zilionis R, Kiner E, Klein AM, Mathis D, Benoist C. Single-cell gene
701 expression reveals a landscape of regulatory T cell phenotypes shaped by the TCR. Nat Immunol.
702 2018;19(3):291-301. Epub 2018/02/13. doi: 10.1038/s41590-018-0051-0. PubMed PMID:
703 29434354; PubMed Central PMCID: PMCPMC6069633.

704 39. Headley MB, Bins A, Nip A, Roberts EW, Looney MR, Gerard A, Krummel MF.
705 Visualization of immediate immune responses to pioneer metastatic cells in the lung. Nature.
706 2016;531(7595):513-7. Epub 2016/03/17. doi: 10.1038/nature16985. PubMed PMID: 26982733;
707 PubMed Central PMCID: PMCPMC4892380.
708 40. Montoya JG, Liesenfeld O. Toxoplasmosis. The Lancet. 2004;363(9425):1965-76. doi:
709 10.1016/s0140-6736(04)16412-x.
710 41. Parker SJ RC, Alexander J. CD8+ T cells are the major lymphocyte subpopulation
711 involved in the protective immune response to Toxoplasma gondii in mice. Clin Exp Immunol.
712 1991;84(2):207-12. doi: 10.1111/j.1365-2249.1991.tb08150.x.
713 42. Hunter CA, Sibley LD. Modulation of innate immunity by Toxoplasma gondii virulence
714 effectors. Nat Rev Microbiol. 2012;10(11):766-78. Epub 2012/10/17. doi: 10.1038/nrmicro2858.
715 PubMed PMID: 23070557; PubMed Central PMCID: PMCPMC3689224.
716 43. Frickel EM, Hunter CA. Lessons from Toxoplasma: Host responses that mediate parasite
717 control and the microbial effectors that subvert them. J Exp Med. 2021;218(11). Epub 2021/10/21.
718 doi: 10.1084/jem.20201314. PubMed PMID: 34670268; PubMed Central PMCID:
719 PMCPMC8532566.
720 44. Konradt C, Ueno N, Christian DA, Delong JH, Pritchard GH, Herz J, Bzik DJ, Koshy AA,
721 McGavern DB, Lodoen MB, Hunter CA. Endothelial cells are a replicative niche for entry of
722 Toxoplasma gondii to the central nervous system. Nat Microbiol. 2016;1:16001. Epub 2016/08/31.
723 doi: 10.1038/nmicrobiol.2016.1. PubMed PMID: 27572166; PubMed Central PMCID:
724 PMCPMC4966557.
725 45. Lambert H, Barragan A. Modelling parasite dissemination: host cell subversion and
726 immune evasion by Toxoplasma gondii. Cell Microbiol. 2010;12(3):292-300. Epub 2009/12/10.
727 doi: 10.1111/j.1462-5822.2009.01417.x. PubMed PMID: 19995386.
728 46. Courret N, Darche S, Sonigo P, Milon G, Buzoni-Gatel D, Tardieux I. CD11c- and CD11b-
729 expressing mouse leukocytes transport single Toxoplasma gondii tachyzoites to the brain. Blood.

730 2006;107(1):309-16. Epub 2005/07/30. doi: 10.1182/blood-2005-02-0666. PubMed PMID:
731 16051744; PubMed Central PMCID: PMCPMC1895351.
732 47. Rosenberg A, Sibley LD. Toxoplasma gondii secreted effectors co-opt host repressor
733 complexes to inhibit necroptosis. Cell Host Microbe. 2021;29. Epub 2021/05/28. doi:
734 10.1016/j.chom.2021.04.016. PubMed PMID: 34043960.
735 48. Wang ZD, Liu HH, Ma ZX, Ma HY, Li ZY, Yang ZB, Zhu XQ, Xu B, Wei F, Liu Q.
736 Toxoplasma gondii Infection in Immunocompromised Patients: A Systematic Review and Meta-
737 Analysis. Front Microbiol. 2017;8:389. Epub 2017/03/25. doi: 10.3389/fmicb.2017.00389.
738 PubMed PMID: 28337191; PubMed Central PMCID: PMCPMC5343064.
739 49. Casciotti L, Ely KH, Williams ME, Khan IA. CD8(+)-T-cell immunity against Toxoplasma
740 gondii can be induced but not maintained in mice lacking conventional CD4(+) T cells. Infect
741 Immun. 2002;70(2):434-43. Epub 2002/01/18. doi: 10.1128/iai.70.2.434-443.2002. PubMed
742 PMID: 11796568; PubMed Central PMCID: PMCPMC127655.
743 50. Suzuki Y RJ. The effect of anti-IFN-gamma antibody on the protective effect of Lyt-2+
744 immune T cells against toxoplasmosis in mice. J Immunol. 1990;144(5):1954-6.
745 51. Yap GS SA. Effector cells of both nonhemopoietic and hemopoietic origin are required for
746 interferon (IFN)-gamma- and tumor necrosis factor (TNF)-alpha-dependent host resistance to the
747 intracellular pathogen, Toxoplasma gondii. J Exp Med. 1999;189(7):1083-92. doi:
748 10.1084/jem.189.7.1083.
749 52. Wilson DC, Matthews S, Yap GS. IL-12 signaling drives CD8+ T cell IFN-gamma
750 production and differentiation of KLRG1+ effector subpopulations during Toxoplasma gondii
751 Infection. J Immunol. 2008;180(9):5935-45. Epub 2008/04/22. doi: 10.4049/jimmunol.180.9.5935.
752 PubMed PMID: 18424713.
753 53. Stumhofer JS, Silver JS, Hunter CA. IL-21 is required for optimal antibody production and
754 T cell responses during chronic Toxoplasma gondii infection. PLoS One. 2013;8(5):e62889. Epub

2013/05/15. doi: 10.1371/journal.pone.0062889. PubMed PMID: 23667536; PubMed Central PMCID: PMCPMC3647013.

54. Khan IA, Moretto M, Wei XQ, Williams M, Schwartzman JD, Liew FY. Treatment with soluble interleukin-15Ralpha exacerbates intracellular parasitic infection by blocking the development of memory CD8+ T cell response. J Exp Med. 2002;195(11):1463-70. Epub 2002/06/05. doi: 10.1084/jem.20011915. PubMed PMID: 12045244; PubMed Central PMCID: PMCPMC2193543.

55. Collins MH, Craft JM, Bustamante JM, Tarleton RL. Oral exposure to Trypanosoma cruzi elicits a systemic CD8(+) T cell response and protection against heterotopic challenge. Infect Immun. 2011;79(8):3397-406. Epub 2011/06/02. doi: 10.1128/IAI.01080-10. PubMed PMID: 21628516; PubMed Central PMCID: PMCPMC3147593.

56. John B, Harris TH, Tait ED, Wilson EH, Gregg B, Ng LG, Mrass P, Roos DS, Dzierszinski F, Weninger W, Hunter CA. Dynamic Imaging of CD8(+) T cells and dendritic cells during infection with Toxoplasma gondii. PLoS Pathog. 2009;5(7):e1000505. Epub 2009/07/07. doi: 10.1371/journal.ppat.1000505. PubMed PMID: 19578440; PubMed Central PMCID: PMCPMC2700268.

57. Dupont CD, Christian DA, Selleck EM, Pepper M, Leney-Greene M, Harms Pritchard G, Koshy AA, Wagage S, Reuter MA, Sibley LD, Betts MR, Hunter CA. Parasite fate and involvement of infected cells in the induction of CD4+ and CD8+ T cell responses to Toxoplasma gondii. PLoS Pathog. 2014;10(4):e1004047. Epub 2014/04/12. doi: 10.1371/journal.ppat.1004047. PubMed PMID: 24722202; PubMed Central PMCID: PMCPMC3983043.

58. Salvioni A, Belloy M, Lebourg A, Bassot E, Cantaloube-Ferrieu V, Vasseur V, Blanie S, Liblau RS, Suberbielle E, Robey EA, Blanchard N. Robust Control of a Brain-Persisting Parasite through MHC I Presentation by Infected Neurons. Cell Rep. 2019;27(11):3254-68 e8. Epub 2019/06/13. doi: 10.1016/j.celrep.2019.05.051. PubMed PMID: 31189109.

780 59. Pepper M, Dzierszinski F, Crawford A, Hunter CA, Roos D. Development of a system to
781 study CD4+-T-cell responses to transgenic ovalbumin-expressing Toxoplasma gondii during
782 toxoplasmosis. Infect Immun. 2004;72(12):7240-6. Epub 2004/11/24. doi:
783 10.1128/IAI.72.12.7240-7246.2004. PubMed PMID: 15557649; PubMed Central PMCID:
784 PMCPMC529136.
785 60. Gregg B, Dzierszinski F, Tait E, Jordan KA, Hunter CA, Roos DS. Subcellular antigen
786 location influences T-cell activation during acute infection with Toxoplasma gondii. PLoS One.
787 2011;6(7):e22936. Epub 2011/08/11. doi: 10.1371/journal.pone.0022936. PubMed PMID:
788 21829561; PubMed Central PMCID: PMCPMC3145783.
789 61. Tait ED, Jordan KA, Dupont CD, Harris TH, Gregg B, Wilson EH, Pepper M, Dzierszinski
790 F, Roos DS, Hunter CA. Virulence of Toxoplasma gondii is associated with distinct dendritic cell
791 responses and reduced numbers of activated CD8+ T cells. J Immunol. 2010;185(3):1502-12.
792 Epub 2010/07/02. doi: 10.4049/jimmunol.0903450. PubMed PMID: 20592284; PubMed Central
793 PMCID: PMCPMC3039871.
794 62. Lee Y, Sasai M, Ma JS, Sakaguchi N, Ohshima J, Bando H, Saitoh T, Akira S, Yamamoto
795 M. p62 Plays a Specific Role in Interferon-gamma-Induced Presentation of a Toxoplasma
796 Vacuolar Antigen. Cell Rep. 2015;13(2):223-33. Epub 2015/10/07. doi:
797 10.1016/j.celrep.2015.09.005. PubMed PMID: 26440898.
798 63. Smith-Garvin JE, Burns JC, Gohil M, Zou T, Kim JS, Maltzman JS, Wherry EJ, Koretzky
799 GA, Jordan MS. T-cell receptor signals direct the composition and function of the memory CD8+
800 T-cell pool. Blood. 2010;116(25):5548-59. Epub 2010/09/18. doi: 10.1182/blood-2010-06-
801 292748. PubMed PMID: 20847203; PubMed Central PMCID: PMCPMC3031403.
802 64. Khan TN, Mooster JL, Kilgore AM, Osborn JF, Nolz JC. Local antigen in nonlymphoid
803 tissue promotes resident memory CD8+ T cell formation during viral infection. J Exp Med.
804 2016;213(6):951-66. Epub 2016/05/25. doi: 10.1084/jem.20151855. PubMed PMID: 27217536;
805 PubMed Central PMCID: PMCPMC4886364.

806 65. Harris TH, Banigan EJ, Christian DA, Konradt C, Tait Wojno ED, Norose K, Wilson EH,
807 John B, Weninger W, Luster AD, Liu AJ, Hunter CA. Generalized Levy walks and the role of
808 chemokines in migration of effector CD8+ T cells. Nature. 2012;486(7404):545-8. Epub
809 2012/06/23. doi: 10.1038/nature11098. PubMed PMID: 22722867; PubMed Central PMCID:
810 PMCPMC3387349.
811 66. Xiao Z, Casey KA, Jameson SC, Curtsinger JM, Mescher MF. Programming for CD8 T
812 cell memory development requires IL-12 or type I IFN. J Immunol. 2009;182(5):2786-94. Epub
813 2009/02/24. doi: 10.4049/jimmunol.0803484. PubMed PMID: 19234173; PubMed Central
814 PMCID: PMCPMC2648124.
815 67. Kaech SM, Tan JT, Wherry EJ, Konieczny BT, Surh CD, Ahmed R. Selective expression
816 of the interleukin 7 receptor identifies effector CD8 T cells that give rise to long-lived memory
817 cells. Nat Immunol. 2003;4(12):1191-8. Epub 2003/11/20. doi: 10.1038/ni1009. PubMed PMID:
818 14625547.
819 68. Tsitsiklis A, Bangs DJ, Robey EA. CD8(+) T Cell Responses to Toxoplasma gondii:
820 Lessons from a Successful Parasite. Trends Parasitol. 2019;35(11):887-98. Epub 2019/10/12.
821 doi: 10.1016/j.pt.2019.08.005. PubMed PMID: 31601477.
822 69. Harms Pritchard G, Hall AO, Christian DA, Wagage S, Fang Q, Muallem G, John B,
823 Glatman Zaretsky A, Dunn WG, Perrigoue J, Reiner SL, Hunter CA. Diverse roles for T-bet in the
824 effector responses required for resistance to infection. J Immunol. 2015;194(3):1131-40. Epub
825 2015/01/04. doi: 10.4049/jimmunol.1401617. PubMed PMID: 25556247; PubMed Central
826 PMCID: PMCPMC4297724.
827 70. Jordan KA, Dupont CD, Tait ED, Liou HC, Hunter CA. Role of the NF-kappaB transcription
828 factor c-Rel in the generation of CD8+ T-cell responses to Toxoplasma gondii. Int Immunol.
829 2010;22(11):851-61. Epub 2010/12/02. doi: 10.1093/intimm/dxq439. PubMed PMID: 21118906;
830 PubMed Central PMCID: PMCPMC2994544.

831 71. Hwang S, Cobb DA, Bhadra R, Youngblood B, Khan IA. Blimp-1-mediated CD4 T cell
832 exhaustion causes CD8 T cell dysfunction during chronic toxoplasmosis. J Exp Med.
833 2016;213(9):1799-818. Epub 2016/08/03. doi: 10.1084/jem.20151995. PubMed PMID:
834 27481131; PubMed Central PMCID: PMCPMC4995081.
835 72. Lieberman LA, Banica M, Reiner SL, Hunter CA. STAT1 plays a critical role in the
836 regulation of antimicrobial effector mechanisms, but not in the development of Th1-type
837 responses during toxoplasmosis. J Immunol. 2004;172(1):457-63. Epub 2003/12/23. doi:
838 10.4049/jimmunol.172.1.457. PubMed PMID: 14688355.
839 73. Yu F, Sharma S, Jankovic D, Gurram RK, Su P, Hu G, Li R, Rieder S, Zhao K, Sun B, Zhu
840 J. The transcription factor Bhlhe40 is a switch of inflammatory versus antiinflammatory Th1 cell
841 fate determination. J Exp Med. 2018;215(7):1813-21. Epub 2018/05/19. doi:
842 10.1084/jem.20170155. PubMed PMID: 29773643; PubMed Central PMCID: PMCPMC6028509.
843 74. Zehn D, Lee SY, Bevan MJ. Complete but curtailed T-cell response to very low-affinity
844 antigen. Nature. 2009;458(7235):211-4. Epub 2009/02/03. doi: 10.1038/nature07657. PubMed
845 PMID: 19182777; PubMed Central PMCID: PMCPMC2735344.
846 75. Netherby-Winslow CS, Ayers KN, Lukacher AE. Balancing Inflammation and Central
847 Nervous System Homeostasis: T Cell Receptor Signaling in Antiviral Brain TRM Formation and
848 Function. Front Immunol. 2020;11:624144. Epub 2021/02/16. doi: 10.3389/fimmu.2020.624144.
849 PubMed PMID: 33584727; PubMed Central PMCID: PMCPMC7873445.
850 76. Frost EL, Lukacher AE. The importance of mouse models to define immunovirologic
851 determinants of progressive multifocal leukoencephalopathy. Front Immunol. 2015;5:646. Epub
852 2015/01/21. doi: 10.3389/fimmu.2014.00646. PubMed PMID: 25601860; PubMed Central
853 PMCID: PMCPMC4283601.
854 77. Maru S, Jin G, Schell TD, Lukacher AE. TCR stimulation strength is inversely associated
855 with establishment of functional brain-resident memory CD8 T cells during persistent viral
856 infection. PLoS Pathog. 2017;13(4):e1006318. Epub 2017/04/15. doi:

857 10.1371/journal.ppat.1006318. PubMed PMID: 28410427; PubMed Central PMCID:
858 PMCPMC5406018.
859 78. Casey KA, Fraser KA, Schenkel JM, Moran A, Abt MC, Beura LK, Lucas PJ, Artis D,
860 Wherry EJ, Hogquist K, Vezys V, Masopust D. Antigen-independent differentiation and
861 maintenance of effector-like resident memory T cells in tissues. J Immunol. 2012;188(10):4866-
862 75. Epub 2012/04/17. doi: 10.4049/jimmunol.1200402. PubMed PMID: 22504644; PubMed
863 Central PMCID: PMCPMC3345065.
864 79. Urban SL, Jensen IJ, Shan Q, Pewe LL, Xue H-H, Badovinac VP, Harty JT. Peripherally
865 induced brain tissue–resident memory CD8+ T cells mediate protection against CNS infection.
866 Nature Immunology. 2020. doi: 10.1038/s41590-020-0711-8.
867 80. Prinz M, Priller J. Tickets to the brain: role of CCR2 and CX3CR1 in myeloid cell entry in
868 the CNS. J Neuroimmunol. 2010;224(1-2):80-4. Epub 2010/06/18. doi:
869 10.1016/j.jneuroim.2010.05.015. PubMed PMID: 20554025.
870 81. Splitt SD SS, Valentine KM, Castellanos BE, Curd AB, Hoyer KK, Jensen KDC. PD-L1,
871 TIM-3, and CTLA-4 Blockade Fails To Promote Resistance to Secondary Infection with Virulent
872 Strains of Toxoplasma gondii. Infection and Immunity. 2018;86(9). doi: 10.1128/IAI.00459-18.
873 82. Bhadra R, Gigley JP, Khan IA. PD-1-mediated attrition of polyfunctional memory CD8+ T
874 cells in chronic toxoplasma infection. J Infect Dis. 2012;206(1):125-34. Epub 2012/04/28. doi:
875 10.1093/infdis/jis304. PubMed PMID: 22539813; PubMed Central PMCID: PMCPMC3415930.
876 83. Bhadra R, Gigley JP, Weiss LM, Khan IA. Control of Toxoplasma reactivation by rescue
877 of dysfunctional CD8+ T-cell response via PD-1-PDL-1 blockade. Proc Natl Acad Sci U S A.
878 2011;108(22):9196-201. Epub 2011/05/18. doi: 10.1073/pnas.1015298108. PubMed PMID:
879 21576466; PubMed Central PMCID: PMCPMC3107287.
880 84. Aldridge DL, Phan AT, de Waal Malefyt R, Hunter CA. Limited Impact of the Inhibitory
881 Receptor TIGIT on NK and T Cell Responses during Toxoplasma gondii Infection.

882 Immunohorizons. 2021;5(6):384-94. Epub 2021/06/06. doi: 10.4049/immunohorizons.2100007.
883 PubMed PMID: 34088852.
884 85. DeLong JH, O'Hara Hall A, Rausch M, Moodley D, Perry J, Park J, Phan AT, Beiting DP,
885 Kedl RM, Hill JA, Hunter CA. IL-27 and TCR Stimulation Promote T Cell Expression of Multiple
886 Inhibitory Receptors. Immunohorizons. 2019;3(1):13-25. Epub 2019/07/30. doi:
887 10.4049/immunohorizons.1800083. PubMed PMID: 31356173; PubMed Central PMCID:
888 PMCPMC6994206.
889 86. Shwetank, Frost EL, Mockus TE, Ren HM, Toprak M, Lauver MD, Netherby-Winslow CS,
890 Jin G, Cosby JM, Evavold BD, Lukacher AE. PD-1 Dynamically Regulates Inflammation and
891 Development of Brain-Resident Memory CD8 T Cells During Persistent Viral Encephalitis. Front
892 Immunol. 2019;10:783. Epub 2019/05/21. doi: 10.3389/fimmu.2019.00783. PubMed PMID:
893 31105690; PubMed Central PMCID: PMCPMC6499176.
894 87. Shwetank, Abdelsamed HA, Frost EL, Schmitz HM, Mockus TE, Youngblood BA,
895 Lukacher AE. Maintenance of PD-1 on brain-resident memory CD8 T cells is antigen independent.
896 Immunol Cell Biol. 2017;95(10):953-9. Epub 2017/08/23. doi: 10.1038/icb.2017.62. PubMed
897 PMID: 28829048; PubMed Central PMCID: PMCPMC5698165.
898 88. Prasad S, Hu S, Sheng WS, Chauhan P, Singh A, Lokensgard JR. The PD-1: PD-L1
899 pathway promotes development of brain-resident memory T cells following acute viral
900 encephalitis. J Neuroinflammation. 2017;14(1):82. Epub 2017/04/15. doi: 10.1186/s12974-017-
901 0860-3. PubMed PMID: 28407741; PubMed Central PMCID: PMCPMC5390367.
902 89. Berg RE, Crossley E, Murray S, Forman J. Memory CD8+ T cells provide innate immune
903 protection against Listeria monocytogenes in the absence of cognate antigen. J Exp Med.
904 2003;198(10):1583-93. Epub 2003/11/19. doi: 10.1084/jem.20031051. PubMed PMID:
905 14623912; PubMed Central PMCID: PMCPMC1592647.
906 90. Soudja SM, Ruiz AL, Marie JC, Lauvau G. Inflammatory monocytes activate memory
907 CD8(+) T and innate NK lymphocytes independent of cognate antigen during microbial pathogen

908 invasion. Immunity. 2012;37(3):549-62. Epub 2012/09/04. doi: 10.1016/j.immuni.2012.05.029.
909 PubMed PMID: 22940097; PubMed Central PMCID: PMCPMC3456987.
910 91. Chu T, Tyznik AJ, Roepke S, Berkley AM, Woodward-Davis A, Pattacini L, Bevan MJ,
911 Zehn D, Prlic M. Bystander-activated memory CD8 T cells control early pathogen load in an
912 innate-like, NKG2D-dependent manner. Cell Rep. 2013;3(3):701-8. Epub 2013/03/26. doi:
913 10.1016/j.celrep.2013.02.020. PubMed PMID: 23523350; PubMed Central PMCID:
914 PMCPMC3628815.
915 92. Lindå H HH, Cullheim S, Levinovitz A, Khademi M, Olsson T. Expression of MHC class I
916 and beta2-microglobulin in rat spinal motoneurons: regulatory influences by IFN-gamma and
917 axotomy. Exp Neurol. 1998;150(2):282-95. doi: 10.1006/exnr.1997.6768.
918 93. Shallberg LA, Hunter CA. Long live the king: Toxoplasma gondii nucleomodulin inhibits
919 necroptotic cell death. Cell Host Microbe. 2021;29(7):1165-6. Epub 2021/07/16. doi:
920 10.1016/j.chom.2021.06.010. PubMed PMID: 34265248.
921 94. Berry ASF, Farias Amorim C, Berry CL, Syrett CM, English ED, Beiting DP. An Open-
922 Source Toolkit To Expand Bioinformatics Training in Infectious Diseases. mBio.
923 2021;12(4):e0121421. Epub 2021/07/07. doi: 10.1128/mBio.01214-21. PubMed PMID:
924 34225494; PubMed Central PMCID: PMCPMC8406131.

925

Figure 1

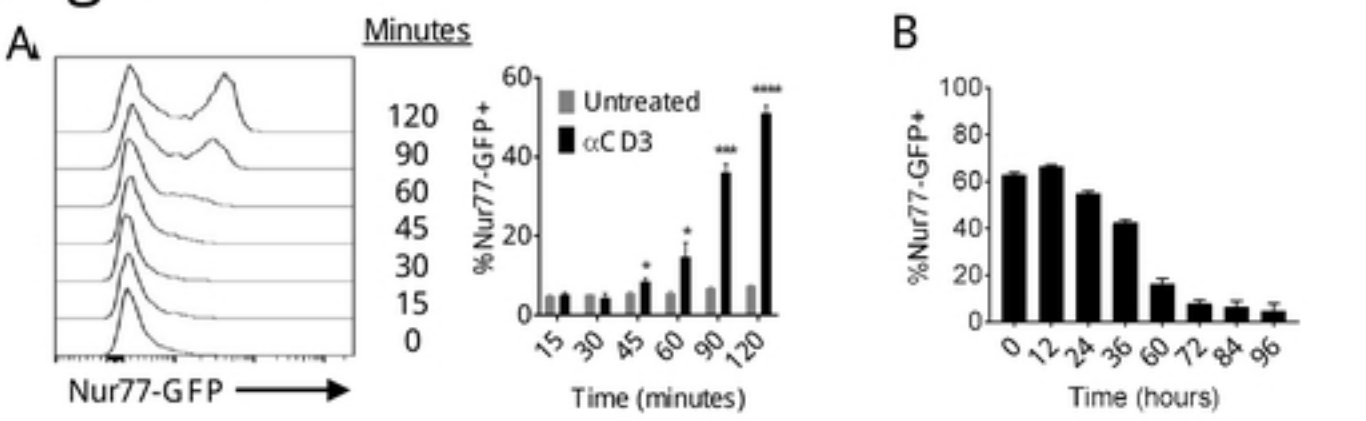

Figure 2

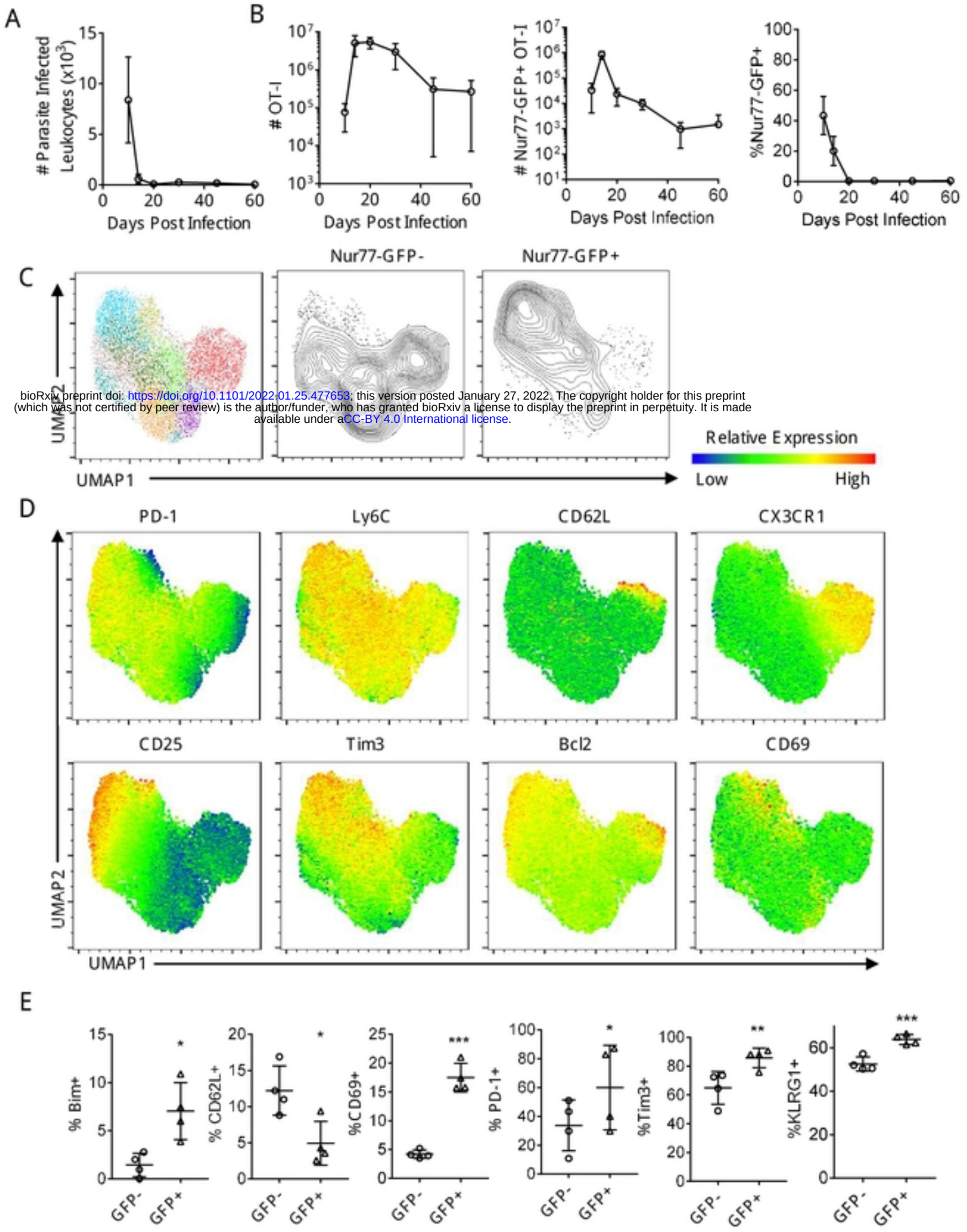

Figure 3

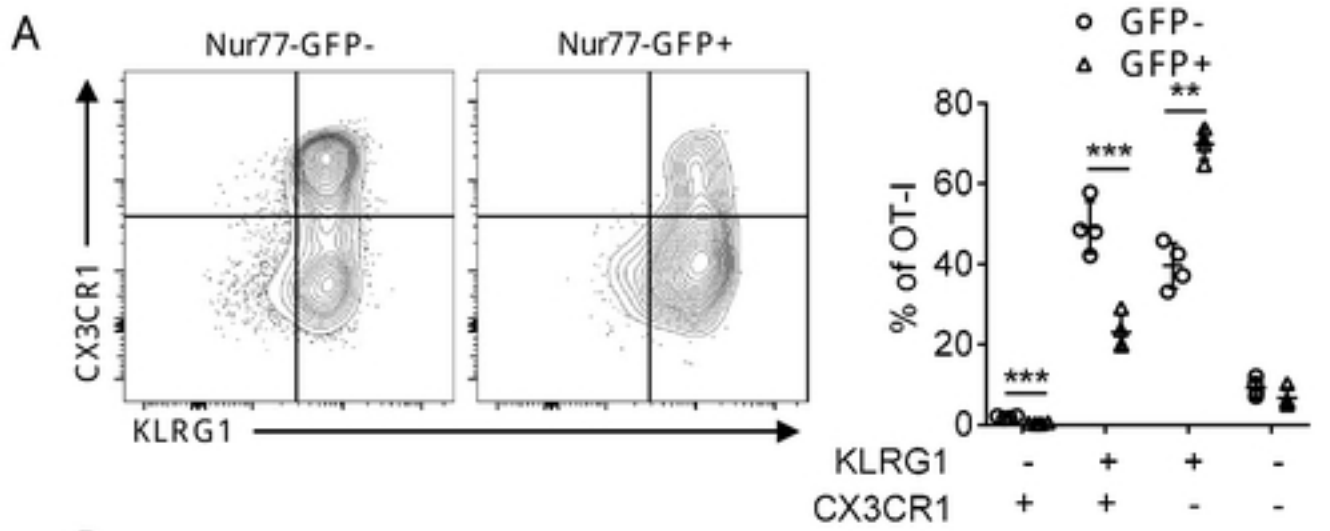

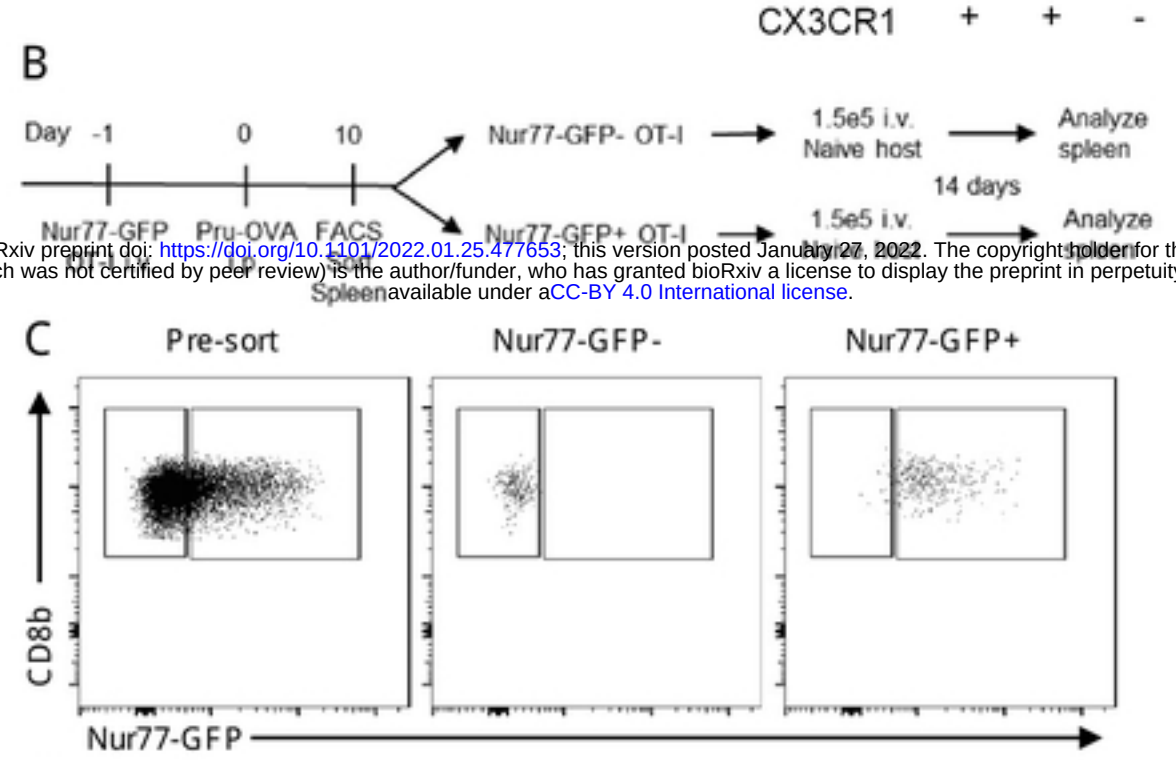

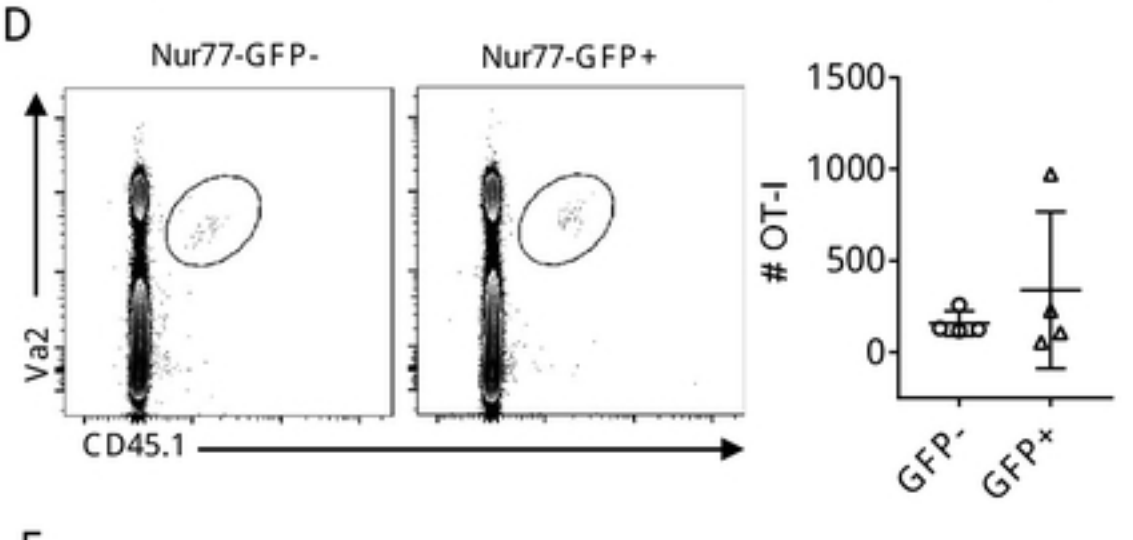

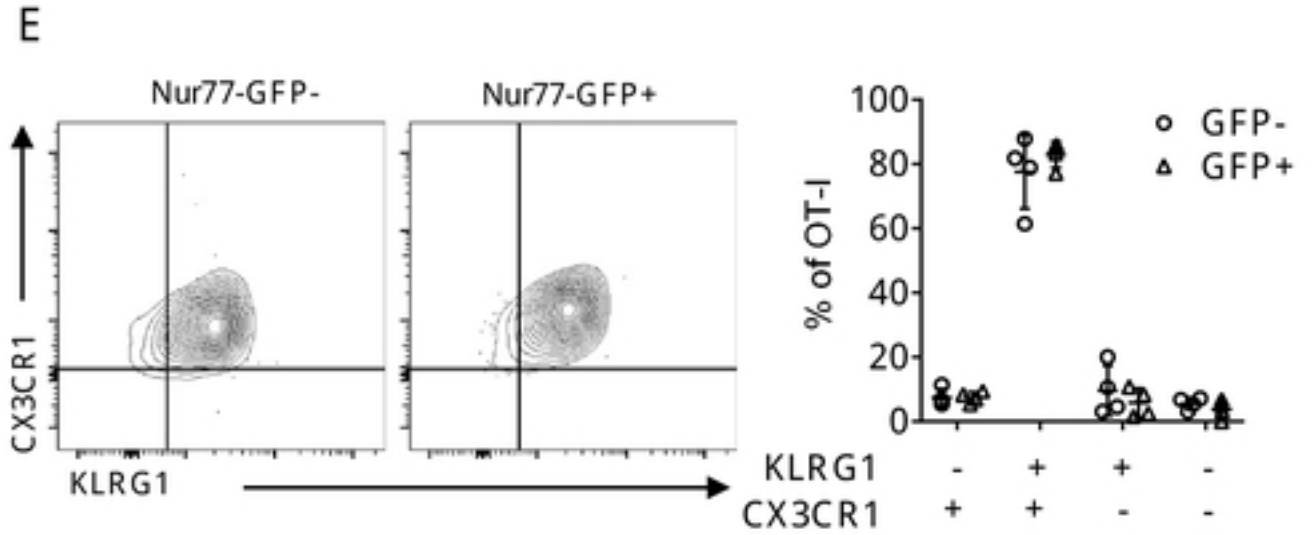

Figure 4

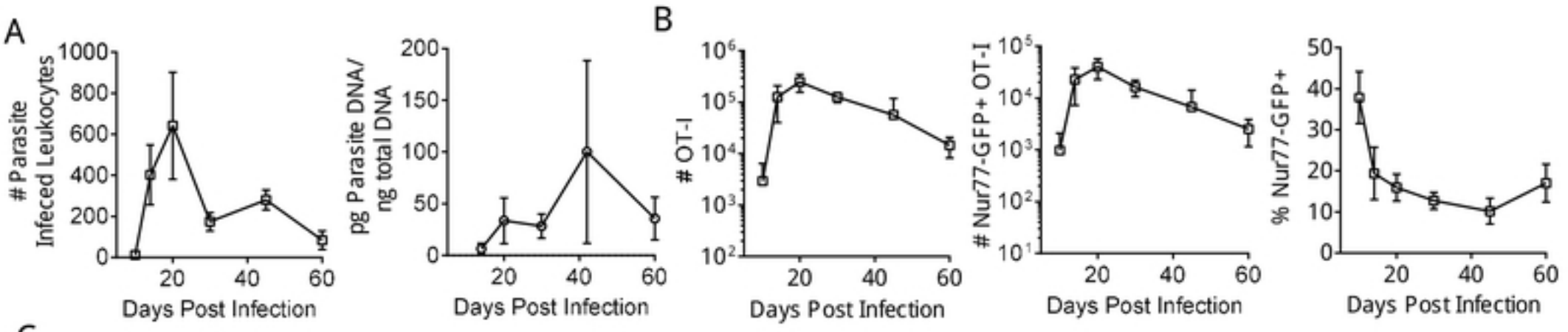

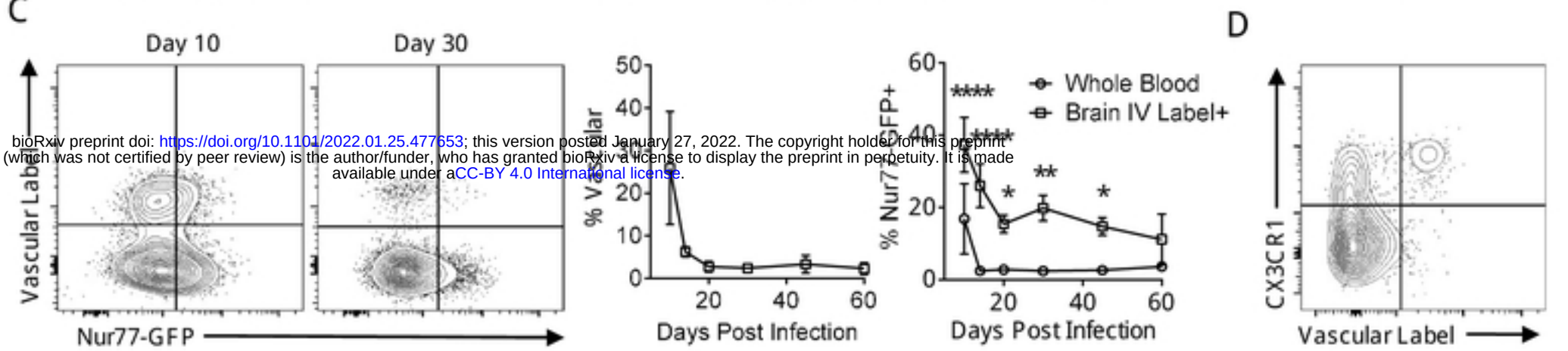

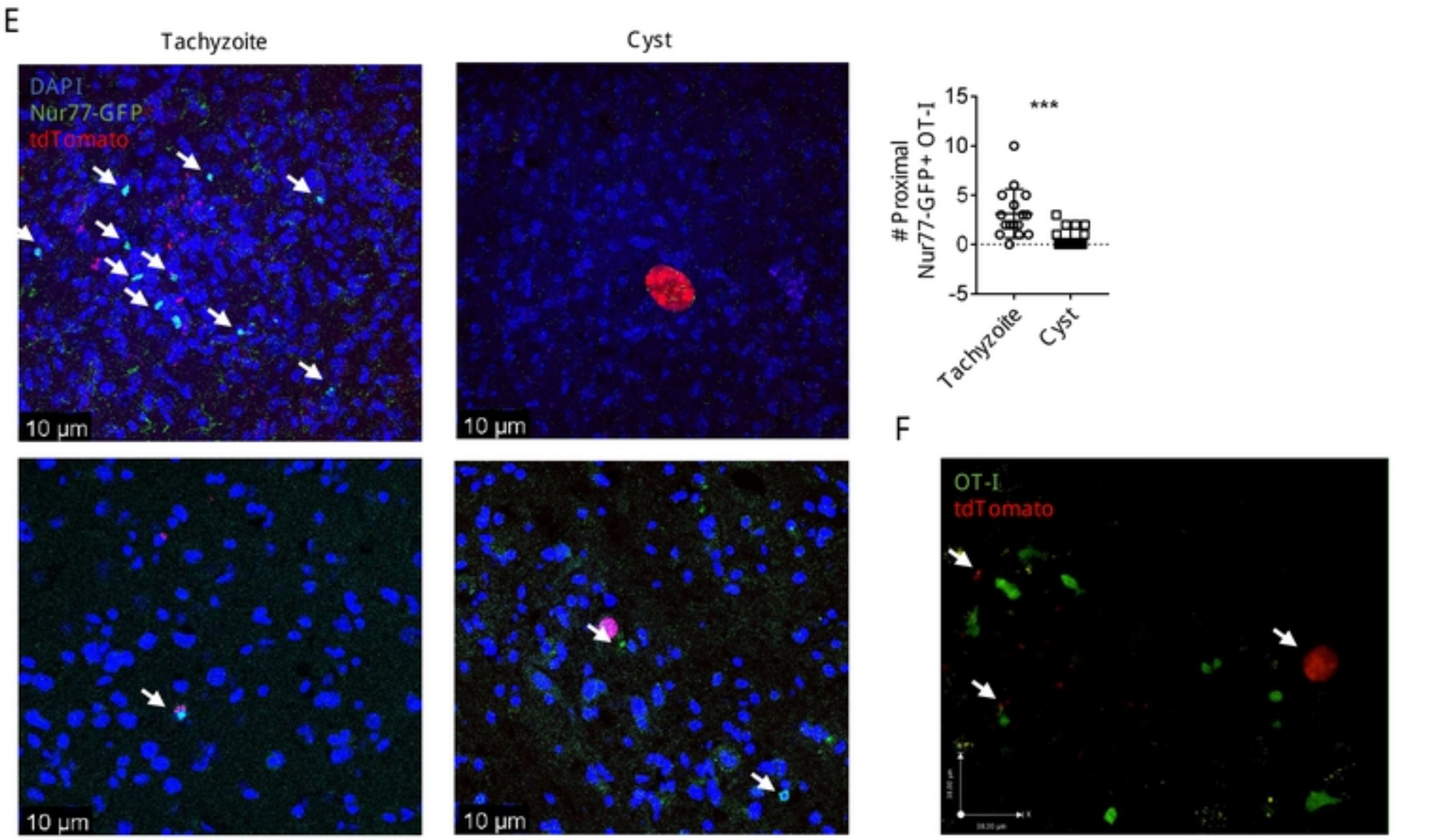

Figure 5

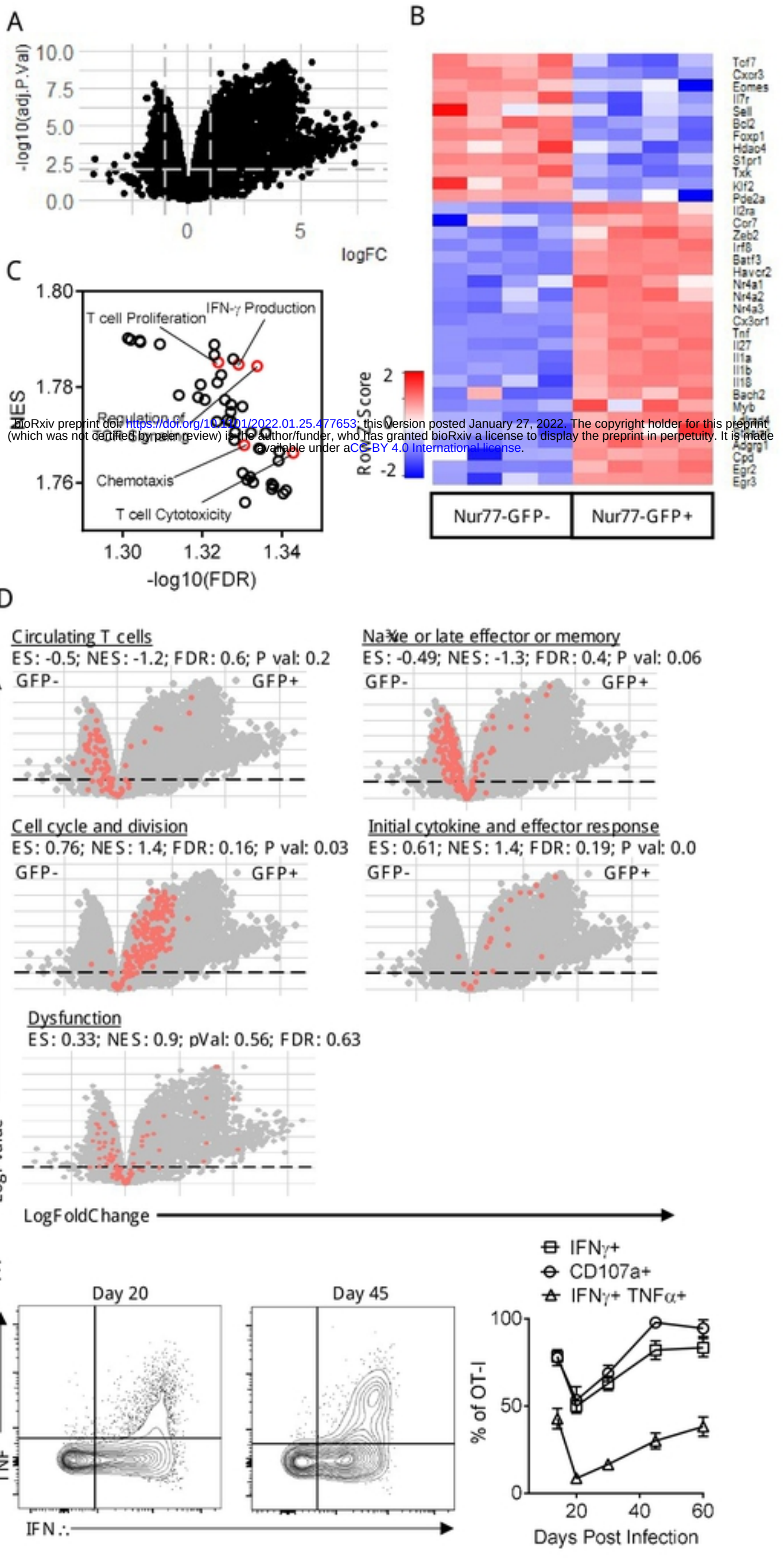

Figure 6

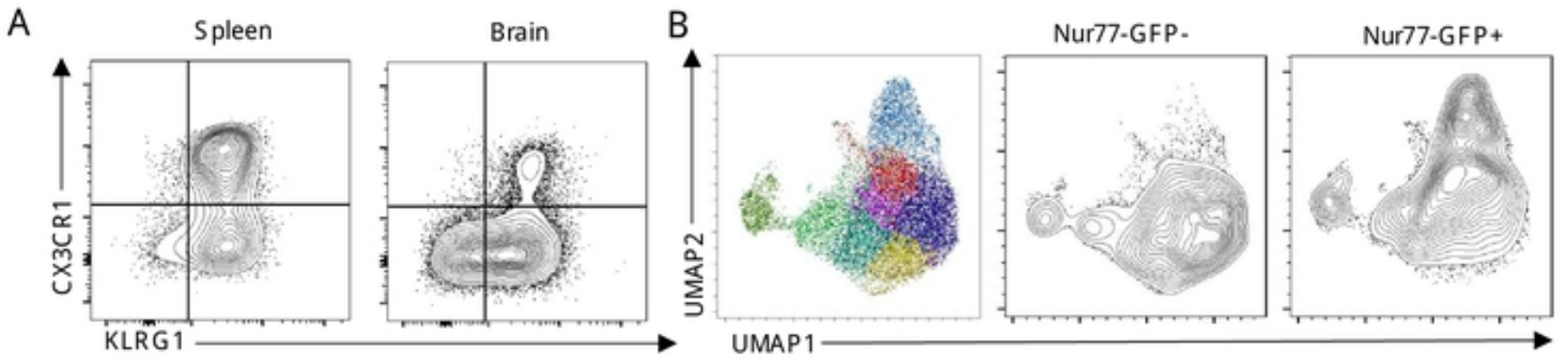

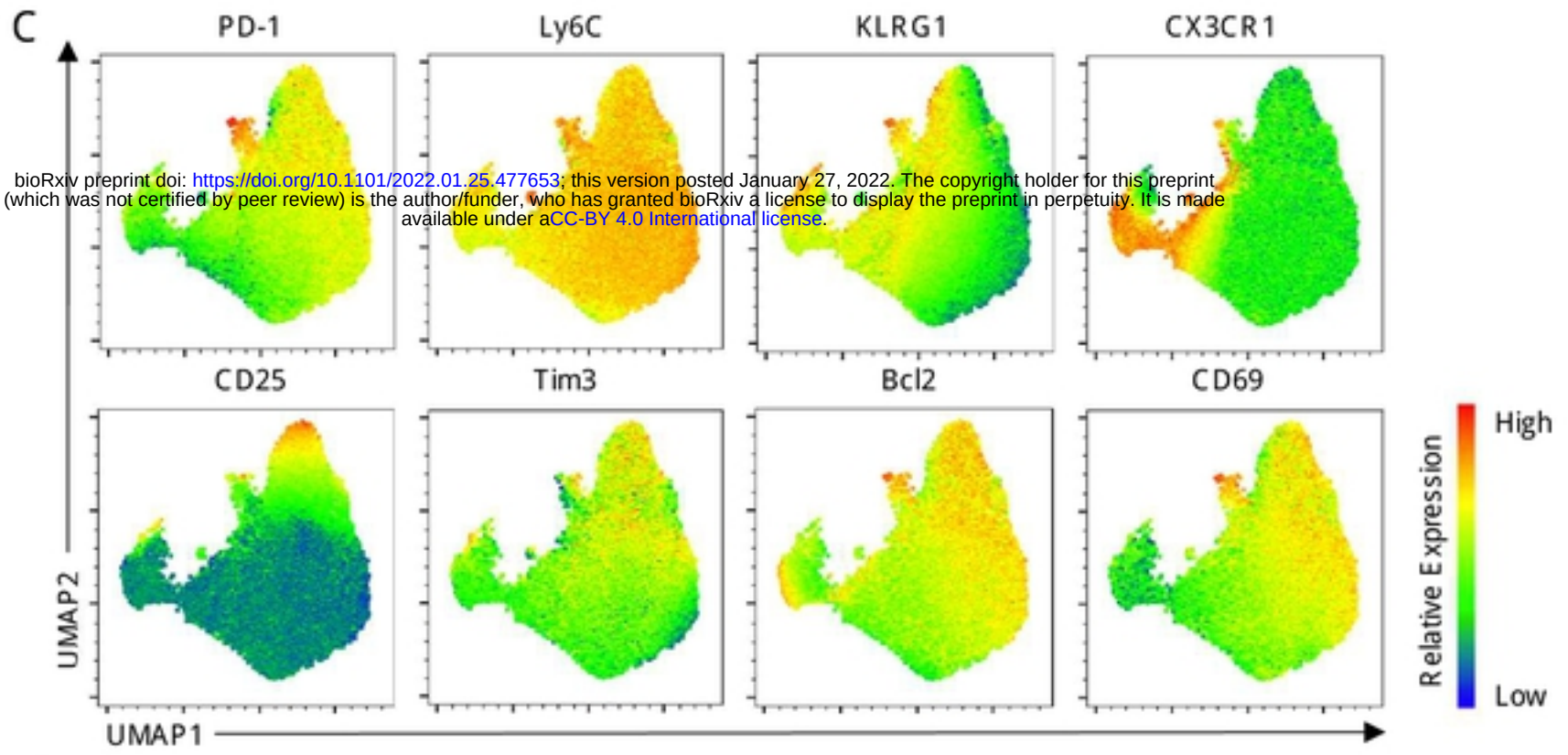

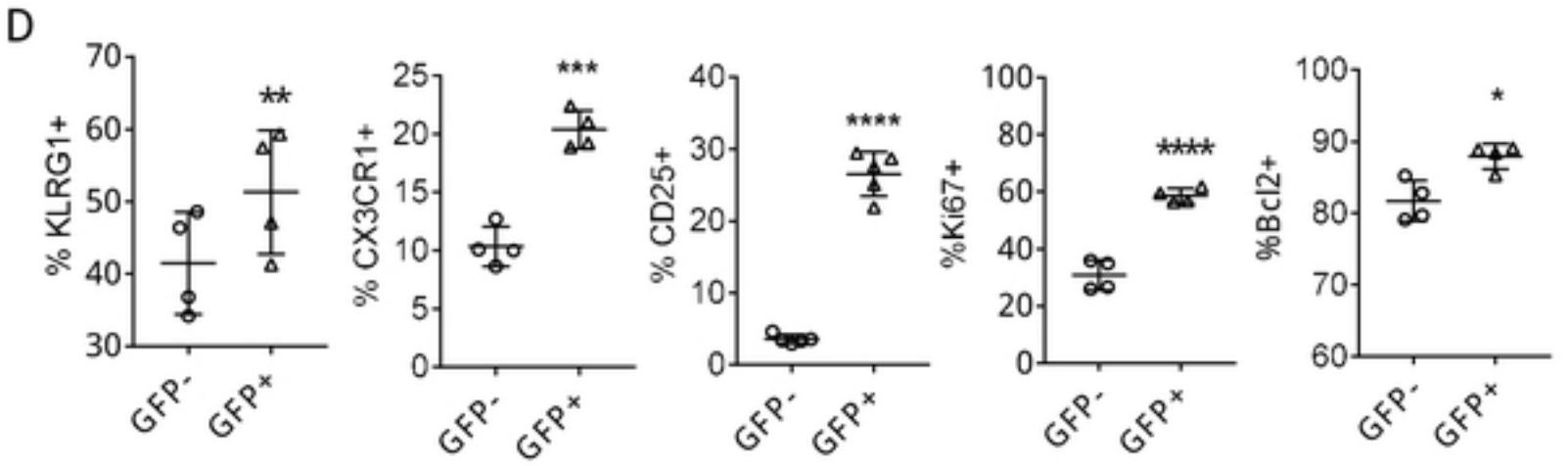

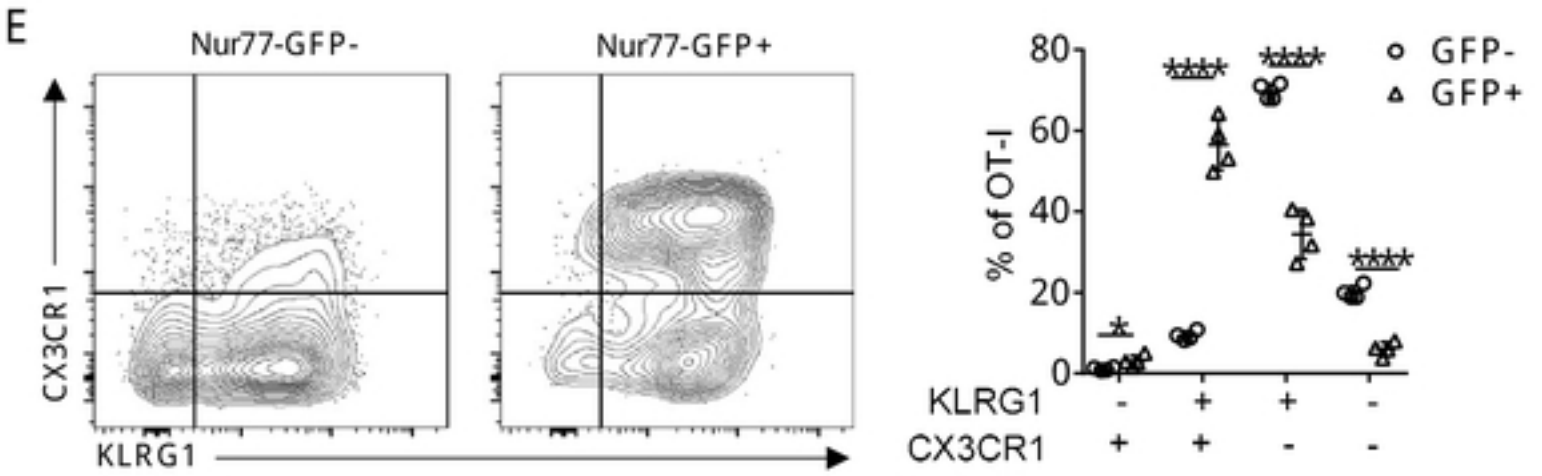

Figure 7

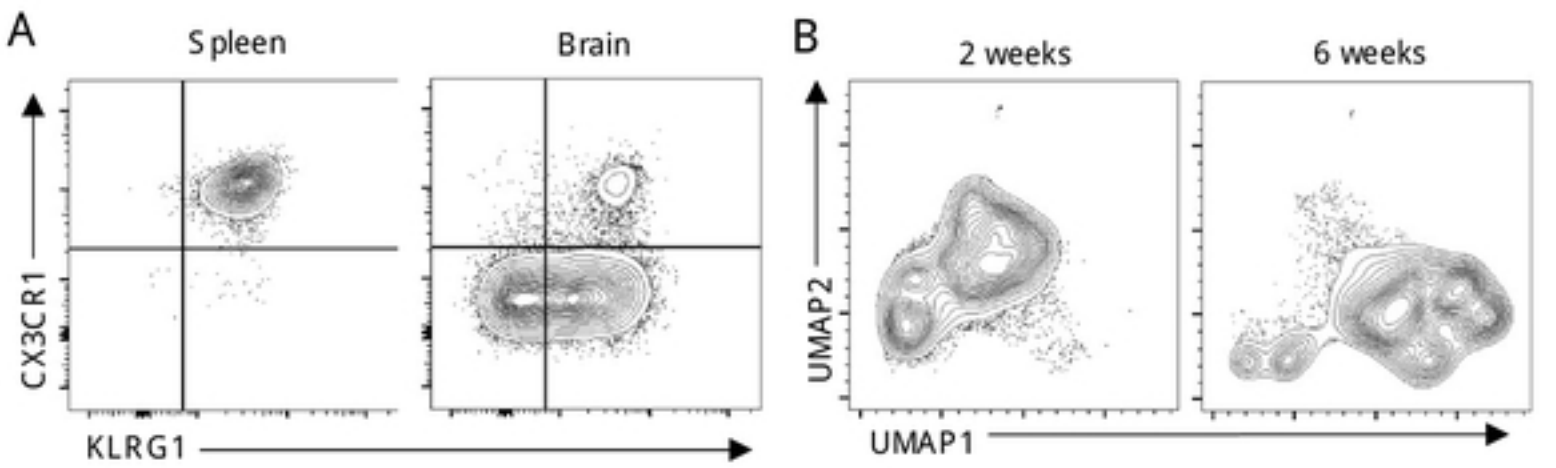

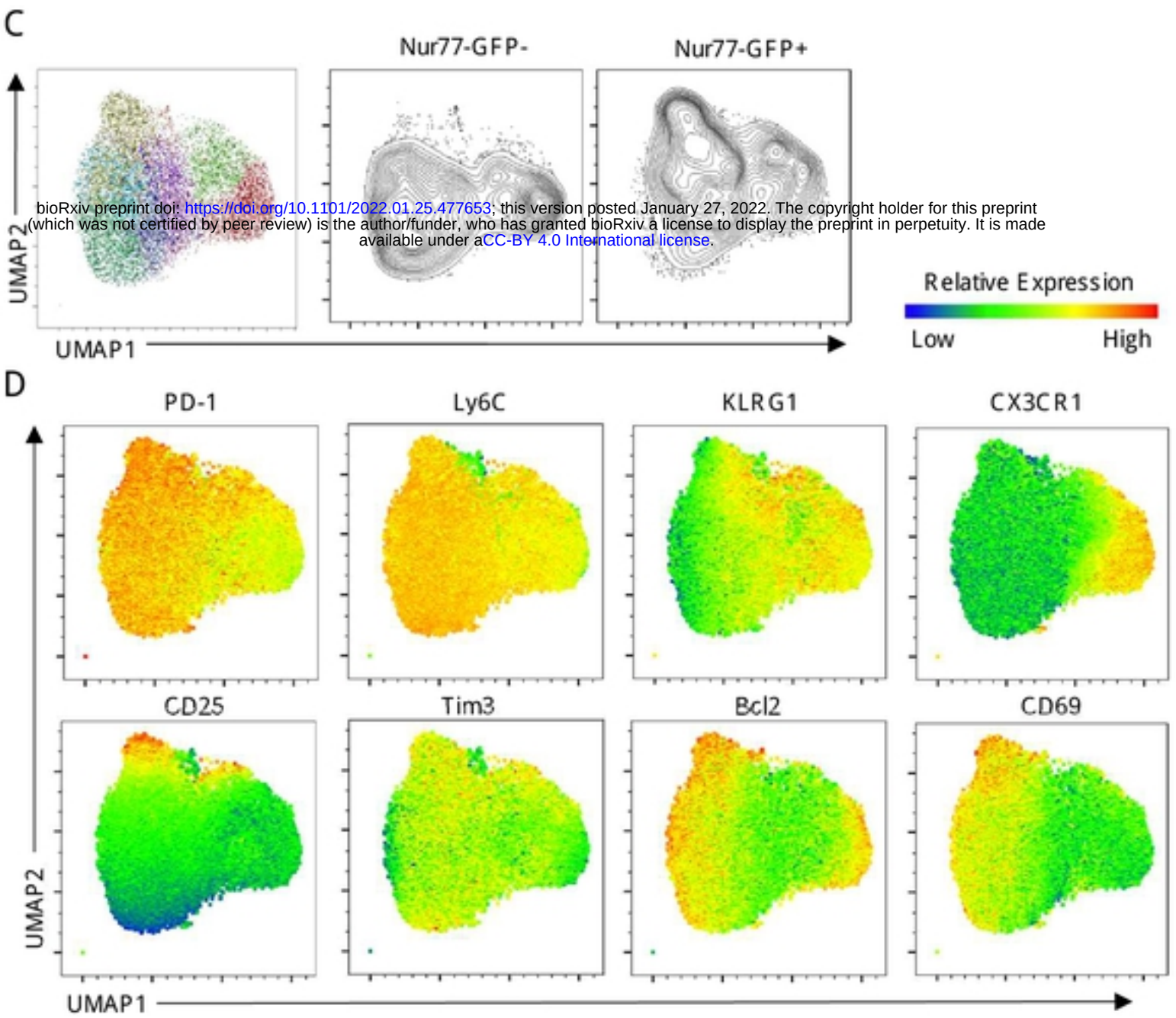

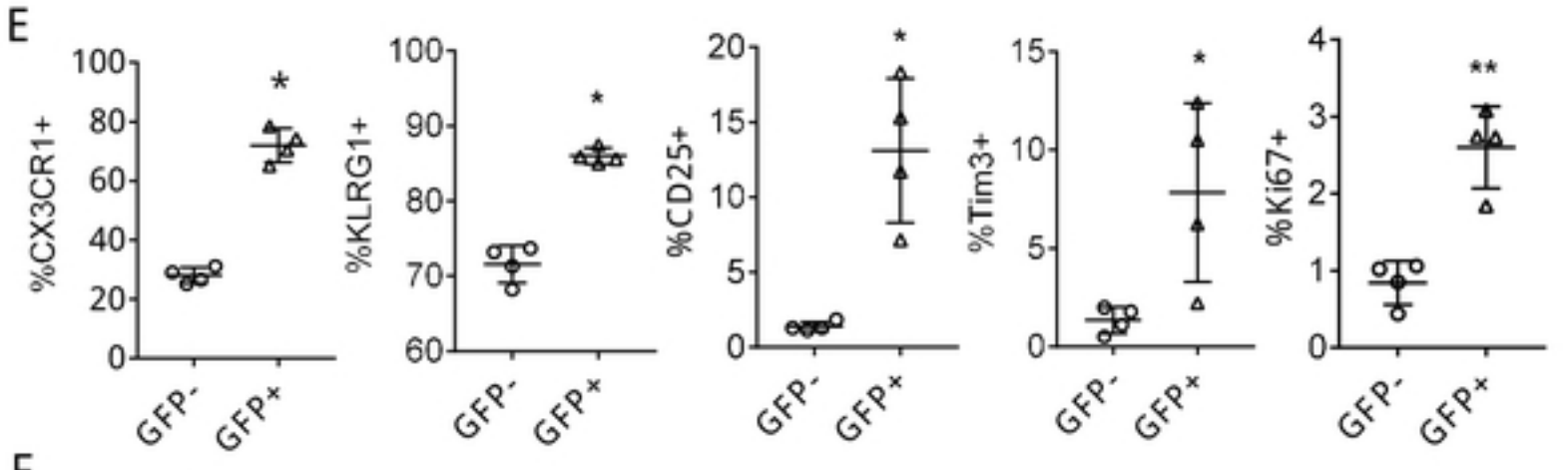

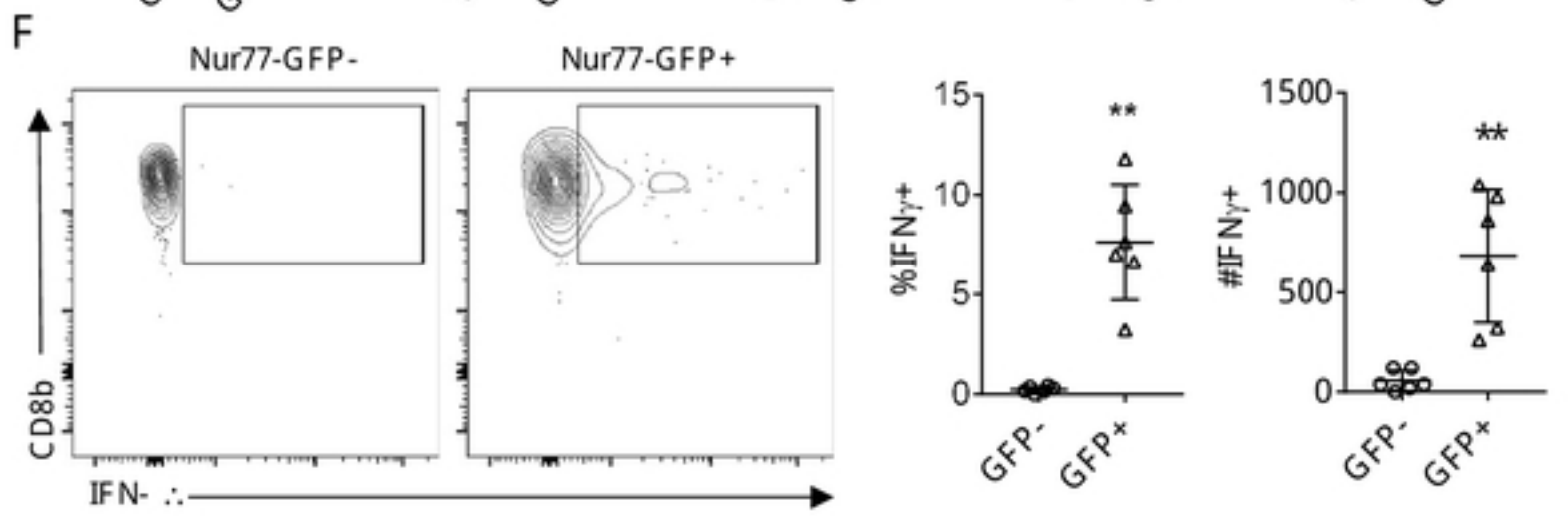

Figure 8

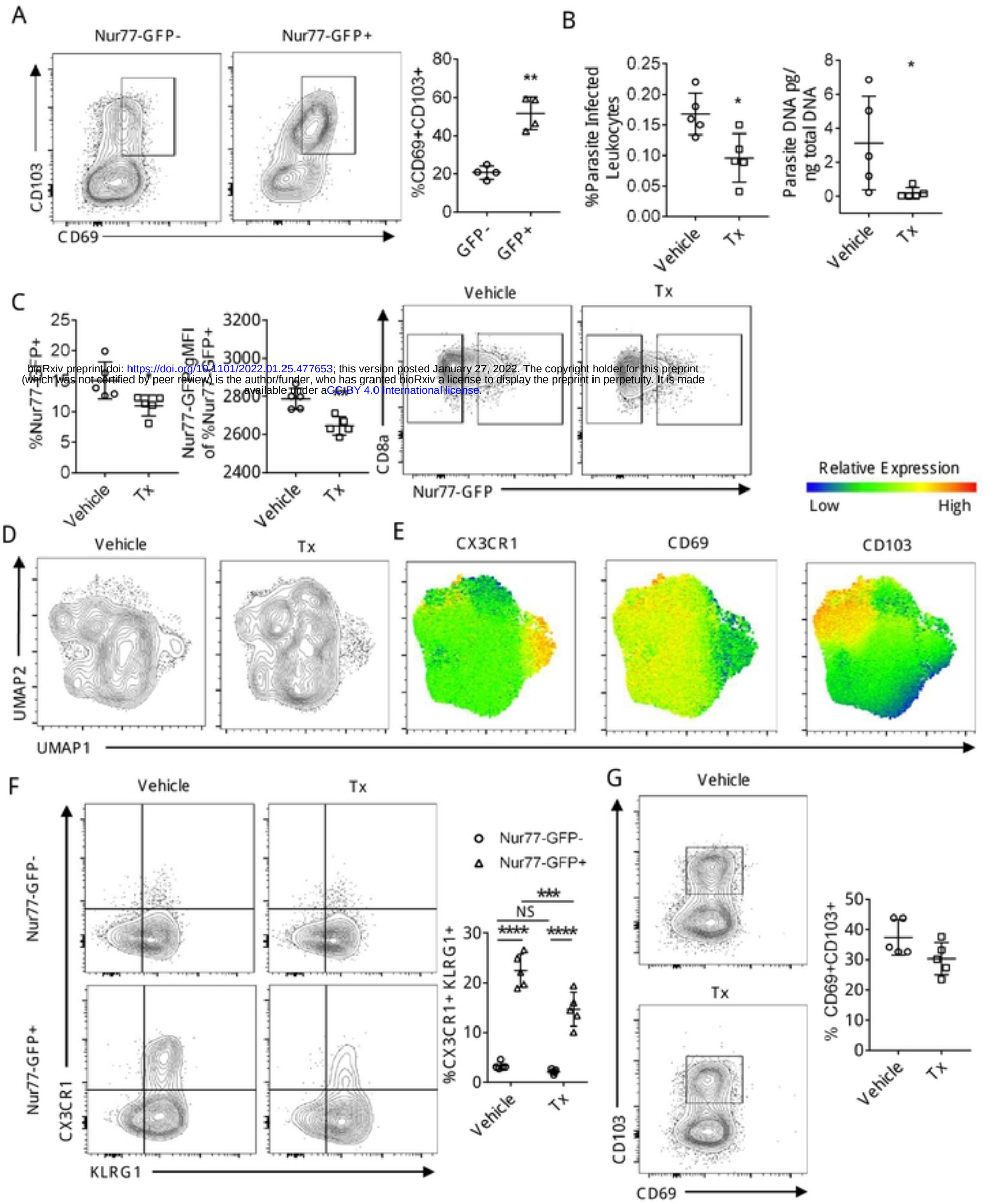

Supplementary Figure 1

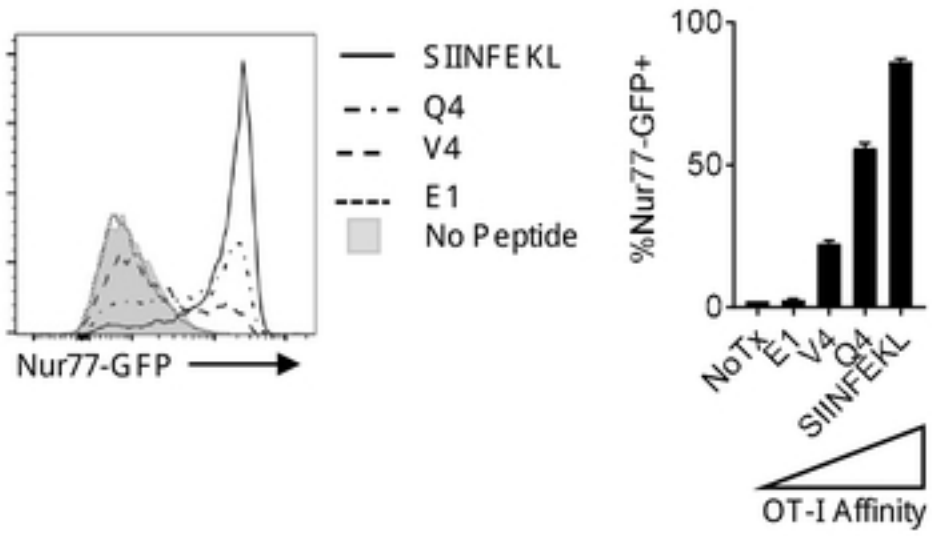

Supplementary Figure 2

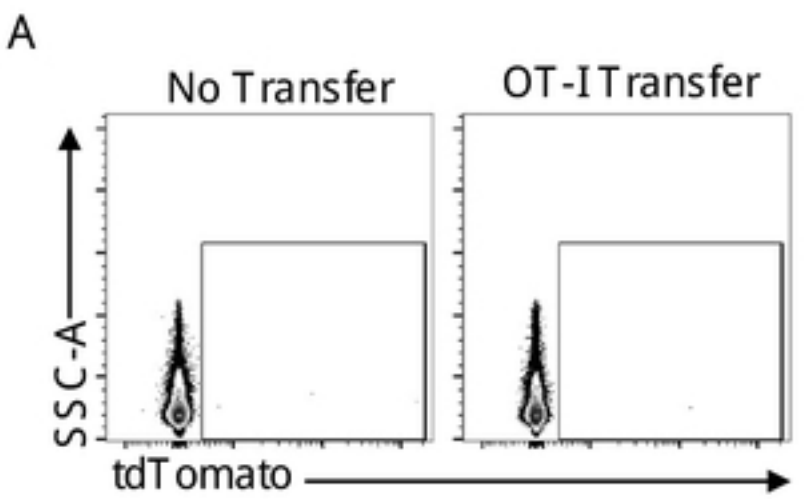

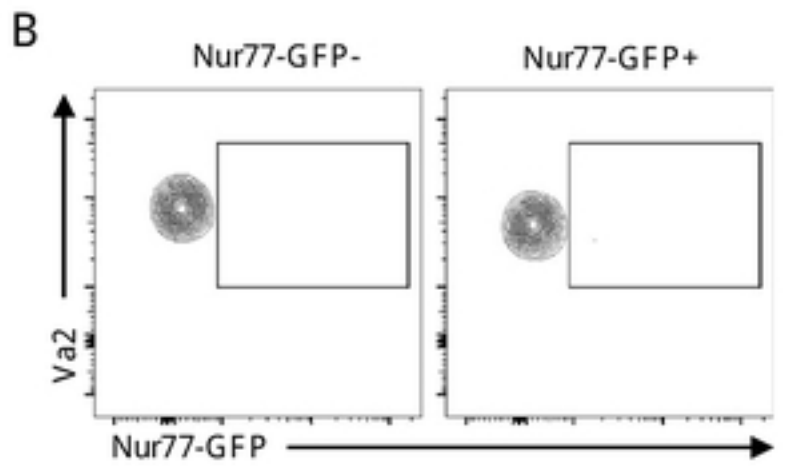

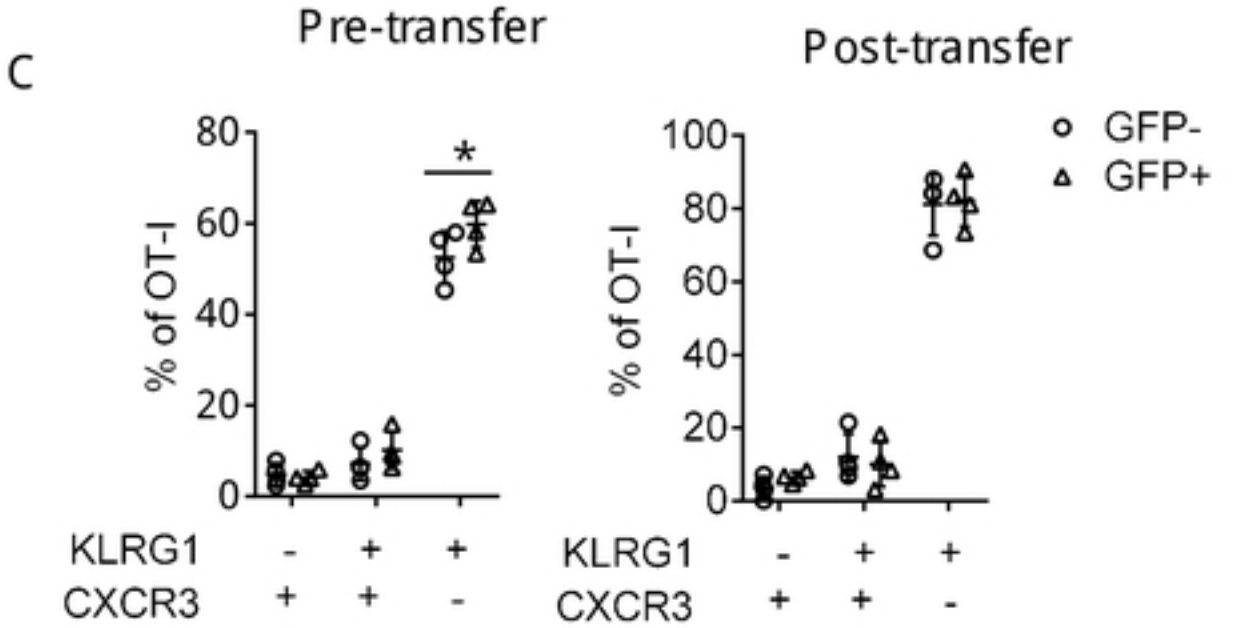

Supplementary Figure 3

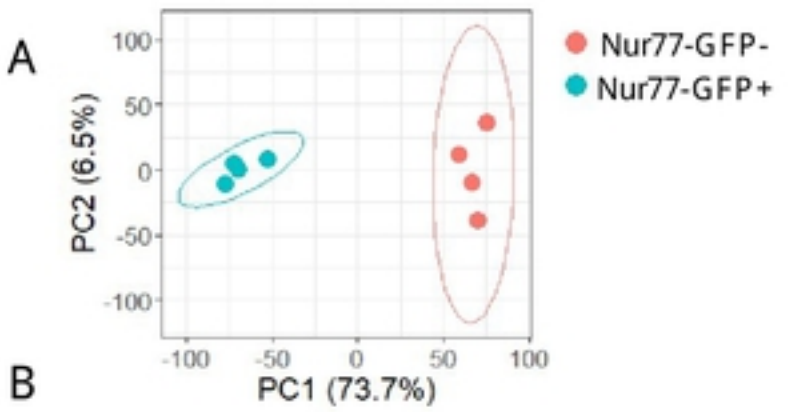

b! a 9	b9{	bha	ix	w
Dh. t×t h{L¤L' 9×w9D- [! ¤Lhb×hC×¤×/ 9[[×a 95L' ¤95×/ Ð¤h¤hÆ/ L¤Ð	ろんさ		れ	ろわあっ
Dh. t×w9D- [! ¤Lhb×hC×a Ð9[hL5×/ 9[[×5LCC9w9b¤L' ¤Lhb	ろんろ		れ	ろわさろ
Dh. t×w9D- [! ¤Lhb×hC×/ 9[[×/ 9[[×! 5I 9{Lhb	ろんろ		れ	ろわあね
Dh. t×w9D- [! ¤Lhb×hC×t 9t ¤L5! {9×! / ¤L' L¤Ð	ろんさ		れ	ろわっあ
Dh. t×t h{L¤L' 9×w9D- [! ¤Lhb×hC×5b! ×. Lb5LbD×¤W b{/ wLt ¤Lhb×C! / ¤hw×! / ¤L' L¤Ð	ろんさ		れ	ろわっわ
Dh. t×w9D- [! ¤Lhb×hC×t b¤LD9b×w9/ 9t ¤hw×a 95L' ¤95×{LDb! [LbD×t! ¤I ° ! Ð	ろんさ		れ	ろわっん
Dh. t×w9D- [! ¤Lhb×hC×{9- Yh/ Ð¤9×/ I 9a h¤! Æ{	ろんれ		れ	ろわわろ
Dh. t×b9D! ¤L' 9×w9D- [! ¤Lhb×hC×{Ða tI h/ Ð¤9×a 95L' ¤95×La a - bL¤Ð	ろんさ		れ	ろわっろ
Dh. t×9Æw/ 9[[- [! w×' 9{L/[9×. LhD9b9{L{	ろんさ		れ	ろわっわ
Dh. t×/ 9[[- [! w×w9{t h b{9×¤h×a 9/ I ! bL/ ! [×{¤La - [- {	ろんさ		れ	ろわっろ
Dh. t×a Ð9{hL5×{9- Yh/ Ð¤9×5LCC9w9b¤L' ¤Lhb	ろんろ		れ	ろわろわ
Dh. t×{9- Yh/ Ð¤9×/ I 9a h¤! Æ{	ろんあっ		れ	ろわわろ
Dh. t×a - [¤L/ 9[[- [! w×hwD! bL{a ! [×{LDb! [LbD	ろんさ		れ	ろわわさ
Dh. t×a Ð9{hL5×59b5wL¤L/ ×/ 9[[×! / ¤L' ! ¤Lhb	ろんろ		れ	ろわわっ
Dh. t×t h{L¤L' 9×w9D- [! ¤Lhb×hC×Lb¤9wC9whb×D! a a ! ×t wh5- / ¤Lhb	ろんさ		れ	ろわわろ
Dh. t×b9- ¤wht I L{×a LDwL ¤Lhb	ろんさ*		れ	ろわっ わ
Dh. t×D9wa Lb! [×/ 9b¤9w×Chwa ! ¤Lhb	ろんさ		れ	ろわろわ
Dh. t×w9D- [! ¤Lhb×hC×w9{t h b{9×¤h×¤- a hw×/ 9[[	ろんさ		れ	ろわろろ
Dh. t×DwL b- [h/ Ð¤9×a LDwL ¤Lhb	ろんわ		れ	ろわんろ
Dh. t×! 5! t¤L' 9×La a - b9×w9{t h b{9	ろんろ		れ	ろわんわ
Dh. t×t h{L¤L' 9×w9D- [! ¤Lhb×hC×t 9t ¤L5! {9×! / ¤L' L¤Ð	ろんわ		れ	ろわんわ
Dh. t×t h{L¤L' 9×w9D- [! ¤Lhb×hC×bC×Y! t t! . ×¤wL b{/ wLt ¤Lhb×C! / ¤hw×! / ¤L' L¤Ð	ろんん		れ	ろわんわ
Dh. t×w9{t h b{9×¤h×¤- a hw×b9/ wh{L{×C! / ¤hw	ろんろ		れ	ろわろろ
Dh. t×t h{L¤L' 9×w9D- [! ¤Lhb×hC×/ Ð{¤9Lb9×¤Ðt 9×9b5h t 9t ¤L5! {9×! / ¤L' L¤Ð	ろんさ		れ	ろわろん
Dh. t×¤×/ 9[[×t wh[LC9wL ¤Lhb	ろんろ		れ	ろわわろ
Dh. t×[9- Yh/ Ð¤9×t wh[LC9wL ¤Lhb	ろんわ		れ	ろわわれ
Dh. t×t h{L¤L' 9×w9D- [! ¤Lhb×hC×a Ð9[hL5×/ 9[[×5LCC9w9b¤L' ¤Lhb	ろんろ*		れ	ろわろろ
Dh. t×w9D- [! ¤Lhb×hC×Lbb! ¤9×La a - b9×w9{t h b{9	ろんん		れ	ろわろん
Dh. t×C/ ×9t{L{h b×w9/ 9t ¤hw×{LDb! [LbD×t! ¤I ° ! Ð	ろんん		れ	ろわろろ
Dh. t×w9D- [! ¤Lhb×hC×b! ¤- wL [×YL{[9w×/ 9[[×a 95L' ¤95×La a - bL¤Ð	ろんろ		れ	ろわろろ
Dh. t×t h{L¤L' 9×w9D- [! ¤Lhb×hC×/ 9[[×! / ¤L' ! ¤Lhb	ろんろ		れ	ろわろん
Dh. t×t h{L¤L' 9×w9D- [! ¤Lhb×hC×La a - b9×9CC9/ ¤hw×t wh/ 9{{	ろんろ		れ	ろわろを
Dh. t×t h{L¤L' 9×w9D- [! ¤Lhb×hC×{9/ w9¤Lhb	ろんろ*		れ	ろわろれ
Dh. t×t h{L¤L' 9×w9D- [! ¤Lhb×hC×I 9a ht h9{L{	ろんろ*		れ	ろわろわ
Dh. t×bC{! a a ! ¤hwÐ×w9{t h b{9	ろんれ		れ	ろわれろ
Dh. t×w9D- [! ¤Lhb×hC×{9- Yh/ Ð¤9×a 95L' ¤95×La a - bL¤Ð	ろれ*		れ	ろわろろ
Dh. t×w9D- [! ¤Lhb×hC×' LwL [×{LC9×/ Ð/ [9	ろんれ		れ	ろわろろ
Dh. t×a Ð9{hL5×{9- Yh/ Ð¤9×! / ¤L' ! ¤Lhb	ろんれ		れ	ろわれを
Dh. t×I - a hwL [×La a - b9×w9{t h b{9	ろをわ		れ	ろわれろ
Dh. t×! [tI ! ×. 9¤! ×¤×/ 9{[×5LCC9w9b¤L' ¤Lhb	ろをん		れ	ろわろろ